PRELIMINARY STUDY OF IN-SITU
MEASUREMENTS OF FRICTION AND BEARING IN CLAY

By
Joseph D. Rehmet
Research Assistant

and

Harry M. Coyle
Associate Research Engineer

Research Report Number 125-3

Bearing Capacity for Axially Loaded Piles
Research Study Number 2-5-67-125

September 1969

TEXAS TRANSPORTATION INSTITUTE
Texas A&M University
College Station, Texas

ABSTRACT

This report presents the results of a series of field tests conducted on several newly developed in-situ testing devices. The in-situ testing devices are to be used to measure static values of skin friction and point bearing during sampling operations with an auger or a core drilling rig. Measured values of skin friction and point bearing taken during sampling operations are compared with the values taken from tests on an 8-foot section of instrumented drill pipe. All tests are conducted at one test site. The soil at the test site is a highly plastic clay. Soil samples are taken during all phases of the test program.

A few dynamic tests are conducted at the test site using one of the in-situ devices which records simultaneous measurements of skin friction and point bearing. Data from the dynamic tests are used to evaluate friction and tip damping constants for the clay soil. The limited dynamic data indicate that soil damping does increase with depth and is a function of overburden pressure.

This study is preliminary in nature because the in-situ devices and testing procedures are in the development stage. Therefore, no definite conclusions are made concerning the application of test results. However, recommendations are made concerning the device and procedure which should be used for future large scale field test programs.

IMPLEMENTATION STATEMENT

This report presents the results of a test program conducted on several newly developed devices for use with core drilling rigs to measure skin friction and point bearing in clays. The study is preliminary in nature because the devices and the test procedures are in the development stage. The research has not progressed to the point that implementation of the results can be started by the Texas Highway Department.

The opinions, findings, and conclusions expressed in this report are those of the authors and not necessarily those of the Bureau of Public Roads.

TABLE OF CONTENTS

LIST OF TABLES

LIST OF FIGURES

NOTATION

The following notation was used in this study:

Q = ultimate static bearing capacity,

A_s = embedded surface area of pile shaft,

f = unit skin friction,

A_p = pile end area,

q = unit point bearing,

w_l = soils liquid limit,

w_p = soils plastic limit,

γ_T = total unit weight (lbs/cf),

w_n = natural moisture content (%),

w_{shear} = moisture content at time of shear test (%),

$P_{dynamic}$ = maximum dynamic resistance,

P_{static} = maximum static resistance,

J' = a viscous friction damping constant (sec/ft),

$\dot{x}$ = velocity of pile segment in any time interval (fps),

N = a power to which the loading velocity is raised, and

J = a viscous tip damping constant (sec/ft).

Chapter I

INTRODUCTION

Nature of the Problem

Since man first utilized the pile as a method of transporting a load to deeper soil stratas which are more capable of sustaining it, he has been concerned with the bearing capacity of these piles. Chellis (3)* enumerates a number of methods and formulas, many empirical in nature, which have been brought forward to predict the load a pile will carry in skin friction and point bearing. None of these have proved entirely satisfactory for one reason or another.

There are presently three methods of predicting the bearing capacity of a pile, as suggested by Bowles (2).

1. A static formula in which the load carried by a pile in skin friction and point bearing are calculated and added to give a static bearing capacity.

2. A dynamic formula which relates the blow count during driving to the static bearing capacity.

3. A full-scale static load test performed at the actual construction site.

The second method is widely considered as an erroneous one and the third method is often very expensive and time consuming. The first method, which uses soil borings and laboratory or in-situ tests seems to be the most practical approach.

The static method of predicting, Q, the ultimate bearing capacity, is based on the following equation:

$$Q = fA_s + qAp \qquad (1)$$

where:

A_s = Embedded surface area of the pile shaft

f   = Unit skin friction,

A_p = Pile end area, and

q   = Unit point bearing.

It would seem that an in-situ device which could make measurement of unit skin friction, f, and unit point bearing, q, would be desirable. Ideally the device and test procedure should fit the following criteria:

1. The device can be utilized during foundation exploration.

2. The test can be run in-situ.

3. It should be simple, reliable, inexpensive to perform, fast, and trouble-free.

4. It can be used to test soft soil materials to hard rock.

---

*Numbers in parenthesis refer to references at the end of this report. "The citations on the following pages follow the style of the **Journal of Soil Mechanics and Foundation Division**," American Society of Civil Engineers.

5. It must provide data which can be correlated with piling and drilled shafts as well as various laboratory data.

Present Status of the Question

According to its Foundation Manual (4), the Texas Highway Department presently utilizes laboratory shear strength tests and the cone penetrometer test to determine bearing capacity of a pile. Sometimes it is impractical or impossible to obtain undisturbed soil samples for laboratory tests. This leaves the cone penetration test as the sole basis of design. Since the cone penetration test is empirical in nature, the data obtained from the test do not give a true indication of the amount of support a pile will gain from skin friction and point bearing. In many cases, the Texas Highway Department also performs full-scale static load tests at a proposed bridge site.

Bauder (1) states that the New Mexico State Highway Commission uses a penetration test which involves a 2⅜-in. diameter pointed pipe. It is driven by a 380-lb ram and is dropped 3 ft. The data obtained are then used with empirical design curves to predict the static bearing capacity of a pile.

As reported by *Railway Engineering and Maintenance* (6), the Southern Railroad uses a miniature pile driving test in which a 1 5/16-in. steel rod with a forged steel point is driven at the test site. After counting the number of blows per foot of penetration, comparison with the pile driving records of full size piles is made to determine the bearing capacity for each foot of penetration.

Prior Research

A literature survey has shown that little research has been done in the area of in-situ measurements of skin friction and point bearing. Schmertmann (7) has done research at the University of Florida recently with an in-situ device known as the Dutch Friction Cone. It is a device which makes separate but non-simultaneous measurement of skin friction and point bearing during a static test.

Objectives

The objectives of this study are:

1. To design and fabricate several testing devices and the equipment necessary to conduct in-situ loading tests during sampling operations.

2. To conduct a field test program at one test site which includes measurement of in-situ skin friction and point bearing during sampling operations and during the static load test on a instrumented drill pipe.

3. To make recommendations, based on the results of this study, concerning the device and procedure which should be used for future field test programs.

Chapter II

TEST EQUIPMENT AND INSTRUMENTATION

General

To carry out the objectives of the study the following equipment was needed:

1. Testing devices,
2. Loading equipment, and
3. Data recording equipment.

The testing devices had to have the capability of being utilized in different configurations and in at least one case, be able to make simultaneous measurement of skin friction and point bearing. For this reason, a device which could accomplish this simultaneous measurement was fabricated and will be called the simultaneous device for the remainder of the report. A second testing device was fabricated which would measure essentially tip-only loads as was a third device which would give a skin friction measurement capability. These will be called the tip-only and skin friction devices, respectively, for the remainder of the report.

The purpose of the loading equipment was essentially threefold: (1) to assist in driving the 8-ft test section of drill pipe, (2) to allow static load tests at different depths, and (3) to allow dynamic load tests at different depths.

The recording equipment was needed to measure strains in the devices and displacement of the devices during static and dynamic load tests.

The Simultaneous Device

This device, capable of simultaneous in-situ measurement of skin friction and point bearing was fashioned after a similar device utilized by Korb (5) (see Figure 1). Essentially it consisted of an outer tubular shaft, and separate inner shaft with a circular tip.

The outer shaft was fabricated from 2.375 in. O.D. 304 stainless steel with a wall thickness of 0.063 in. Four 90 degree Budd SR-4 gage rosettes were mounted 90 degrees apart and 7.5 in. from the bottom of the shaft. These gages were wired to read only axial loads.

The inner shaft was also fabricated of 304 stainless steel. At the tip of the shaft was welded a 0.75-in. thick, 2.23-in. diameter circular section of stainless steel. Four 90 degree Budd SR-4 gage rosettes were mounted on the inner shaft 2.25 in. from the bottom. They were wired in the same manner as the outer shaft. The separation between the outer and inner shafts was sealed by a 1/16-in. C. S. Teflon "O" ring.

Both tubes were connected and aligned with an adapter which in turn was connected to a standard female drill rod coupling. Strain gage leads were brought out through a small hole in the adapter.

The Tip-Only Device

This device (see Figure 2C) was fabricated of 2.735-in. O. D. steel drill pipe. The top 3.75 in. was a standard female drill rod coupling. The bottom 5 in.

was made of the standard drill pipe. The bottom was welded with a 1.0-in. thick steel plate. Four SR-4 Budd gage rosettes were placed 2.13 in. from the bottom of the cell. The walls of the drill pipe were machined to a thickness of .10 in. at the bridge locations in order to produce a specified sensitivity.

The Skin Friction Device

This device (see Figure 2a) was fabricated of 2.375-in. O. D. steel tubing and 2 standard drill rod couplings welded to the tube, male on one end, female
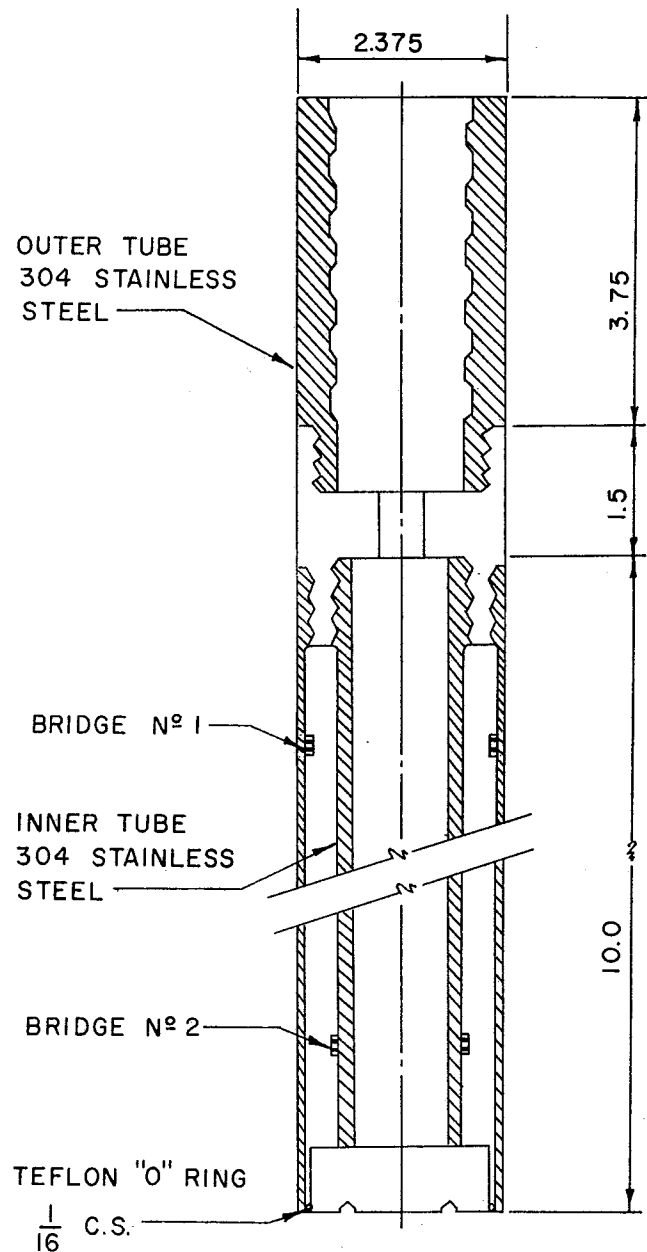
Figure 1. Simultaneous measurement device.
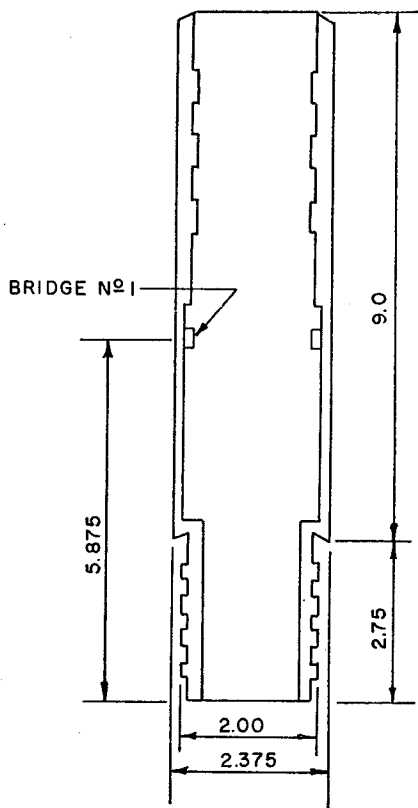
Figure 2a. Skin friction measurement device.
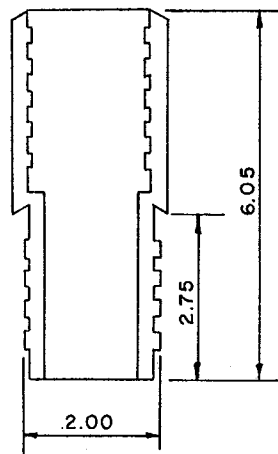
Figure 2b. Spacer.
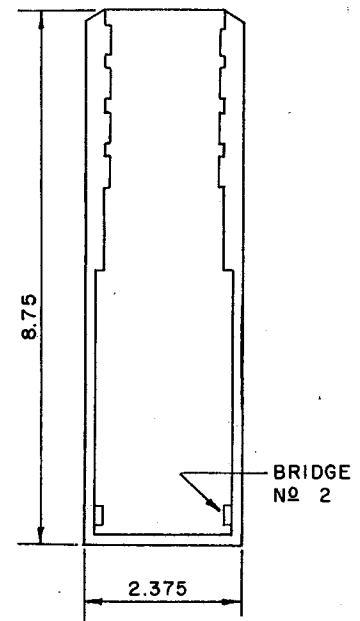
Figure 2c. Tip only measurement device.

on the other. The strain gages were placed 5.88 in. from the bottom of the device. Wall thickness at bridge locations were the same as the tip-only device. As can be seen, the skin friction and tip-only devices were fabricated to be used in interchangeable configurations or together. In order to give a larger area to skin friction measurements when the two were used together, a "spacer" was fabricated (see Figure 2b). It consisted simply of a male and female coupling of the drill pipe welded together. The configurations utilizing the tip-only, skin friction, and "spacer" devices are discussed in greater detail in Chapter IV.

Loading Equipment

The load frame used in the study is shown in Fig. 3. The two vertical members were 6 WF 15.5, 6 feet in length. Twenty-inch by twenty-inch plates were welded to the bottom of each vertical member. Two detachable overlapping plates 2 ft by 6 ft by 0.25 in. were also fabricated to fit around the base of the vertical members. Each was rimmed by 2-in. angle iron and had two 4 ft.-0.75-in. rod arms which allowed them to be bolted to the loading frame. This was to allow for greater weight to be placed on the loading frame during testing due to the fact that static loads in the 4000 lbs to 7000 lb range were expected.

The top horizontal member was fabricated of a 32 in. long 4 WF 13 member with two 6-in. by 6 in. by 0.50-in. plates welded on either end. This member is bolted between the two vertical members. Located in

Figure 3. Load frame.

Figure 4. Driving 8-foot section.

Load Recording Equipment

During static tests, a Budd P-350 strain indicator and a Honeywell 1508 visicorder oscillograph were used to record test data (see Figure 5).

The visicorder was used in conjunction with a linear displacement transducer (see next section) to record pile movement. The Budd strain indicator was used to measure strains in the bridges.

For dynamic tests, the strain gage bridges were hooked into a Model 119 Carrier amplifier. From there, the signals went to the visicorder to record the dynamic loads (see Figure 6). The displacement transducer hook-up was the same as for static tests.
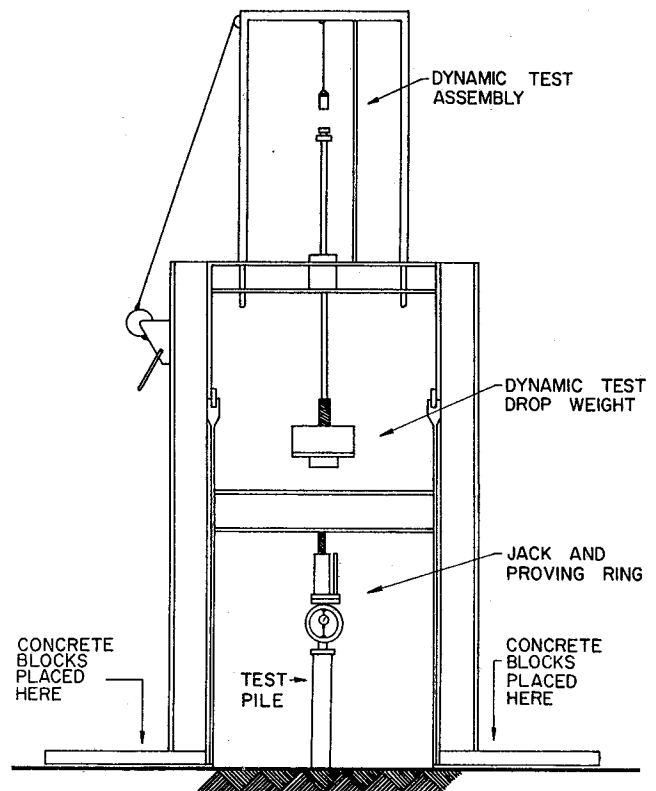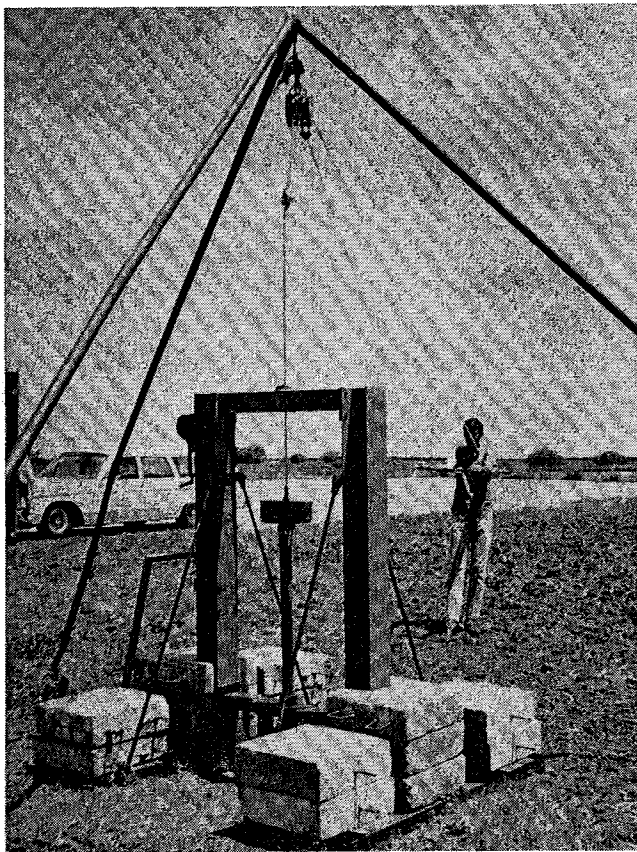
The visicorder utilized light sensitive paper to record data. For static tests a paper speed of 0.1 in. per second was used and for dynamic tests, 80 in. per second.

Displacement Recording Equipment

In order to measure displacements during testing, a Sanborn Model 7DCDT-1000 displacement transducer was used. The transducer is the type which works on the principle that its output signal is directly proportional to the distance traveled of a high flux density permanent magnet through a differentially wound coil.

Figure 5. Static test recording equipment.

the middle of this top horizontal member is a spherical ball bearing through which a 5-ft long, 0.50-in. diameter hardened stainless steel shaft runs. The ball bearing is adjustable to allow for plumbing the shaft. At the bottom end of the shaft was attached an 80-lb weight and a 1.0-in. thick, 3.50-in. diameter steel and rubber striker head. This assembly was used in two capacities: (1) in conjunction with a standard penetration tripod to drive the 8-ft section of drill pipe (see Figure 4), and (2) with a detachable tripling mechanism to perform dynamic tests.

Static load tests were performed by bolting a 6 WF 15.5 horizontal reaction member in place between the two vertical members.

In order to keep the 8-ft section of drill pipe plumb during driving a member was fabricated of a 30-in. by 6.0-in. steel member with a 2.5-in. inside diameter bronze bearing and housing welded in the center through which the pipe was placed during driving.

In order to obtain sufficient weight to load against during testing, forty-five portable reinforced concrete blocks were constructed. These blocks weighed approximately 160 lb. apiece and could be handled easily by two men. These, along with the frame weight, gave a total of approximately 7200 lb.

During the static test, loading was accomplished by an Allstate 5.0-ton hydraulic jack, below which was attached a 10,000-lb capacity proving ring and dial gage used to measure the loads.
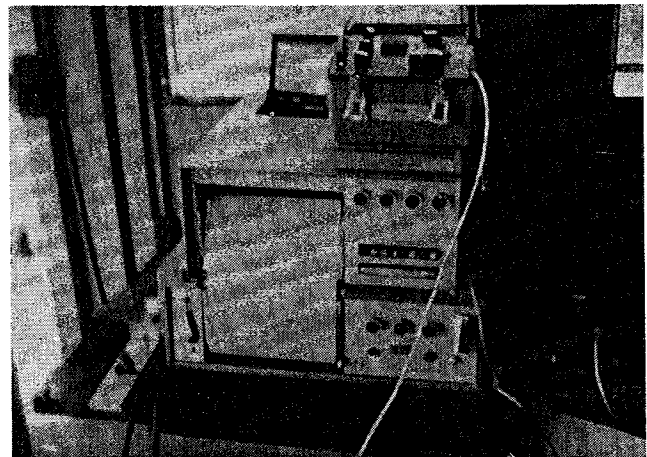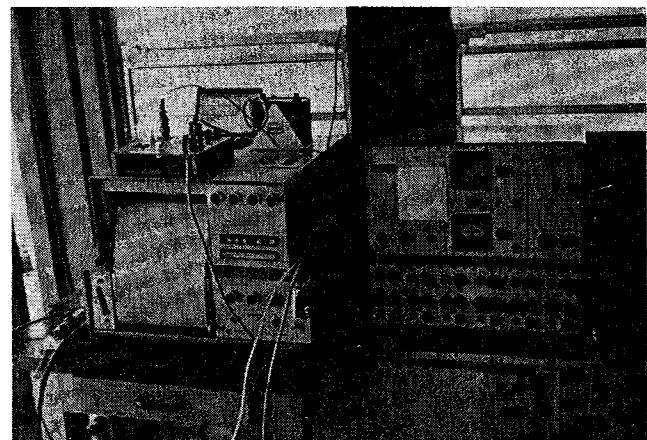

Figure 6. Dynamic test recording equipment.

The transducer was connected to a calibration unit (described in "Calibration" section of this report) and then to the visicorder to report displacements.

A device to which the transducer core could be attached during testing was fabricated. It consisted of a 3.5-in. by 3.5-in. by 2.0-in. block of aluminum having a 2.5-in. hole through the center to allow it to fit over the drill pipe. Four set screws were located in the device to facilitate leveling. Also included on the aluminum block was a 2.0-in. protruding arm with a 1-72 threaded hole into which the core of the displacement transducer was fastened. Schematic diagrams showing the recording and displacement circuits during testing are found in Figures 7 through 10.

Calibration

The load cells were calibrated on an Instron Testing Machine using a Budd P-350 strain indicator (see Figure 11). The tip-only and skin friction devices were loaded to 8,000 lb and the corresponding strains were noted. The simultaneous device was calibrated using a device which allowed the outside shaft to be loaded separately from the inner shaft and vice versa. Readings were taken on the inner shaft during the calibration of the outer shaft and it was found that the load transfer through the Teflon "O" ring was negligible. The results of the calibration tests were plotted and the load versus strain indicator reading curves were obtained for the load cells. It should be noted that the strain gage bridges did exhibit linearity. These calibration curves were used to reduce data from static tests.

L = LONGITUDINAL GAGE
T = TRANSVERSE GAGE

GAGE TYPE
BUDD C6-121-R2TC
$120\Omega \pm .2\Omega$

Figure 8. Load cell circuit.

Since the Honeywell 1508 visicorder and Carrier amplifier system was used for dynamic tests, the load cells were calibrated with this recording device. In order to do this, the bridges were balanced, a known external calibration resistance was plugged into the circuit and a convenient gain was set off on the trace. The resistance was then removed, a known weight was placed on the cell and the galvanometer deflection for

Figure 7. Linear displacement transducer circuit.
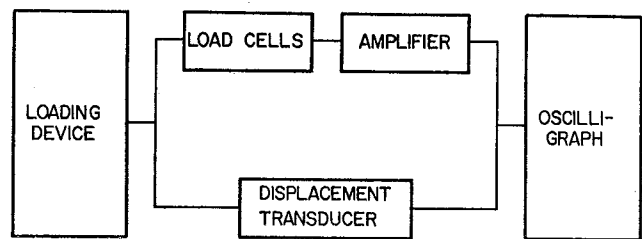
Figure 9. Dynamic test diagram.
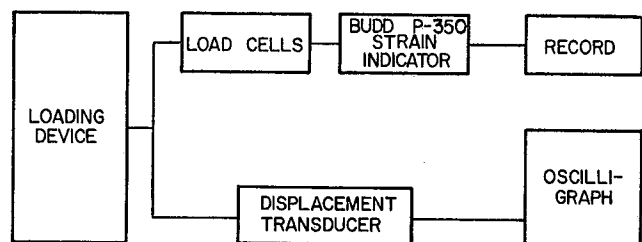
Figure 10. Static test diagram.
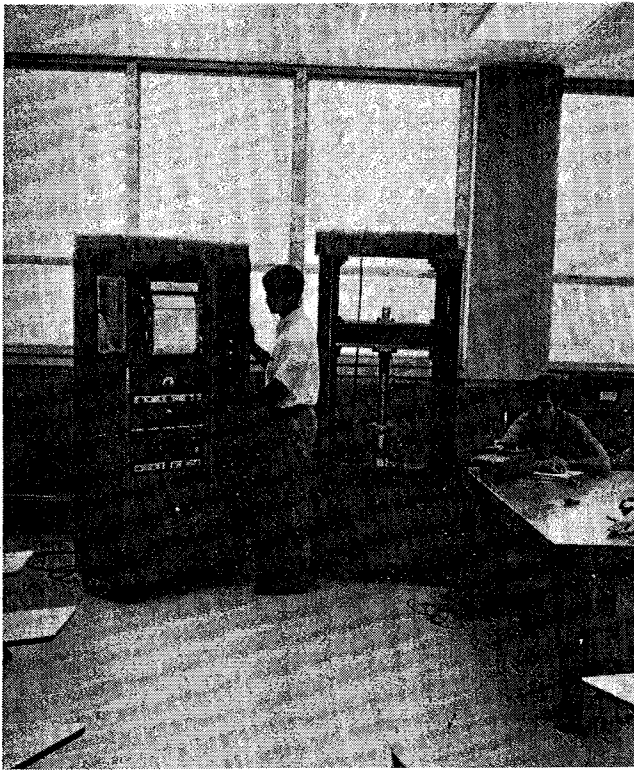
Figure 11. Load cell calibration for static testing.
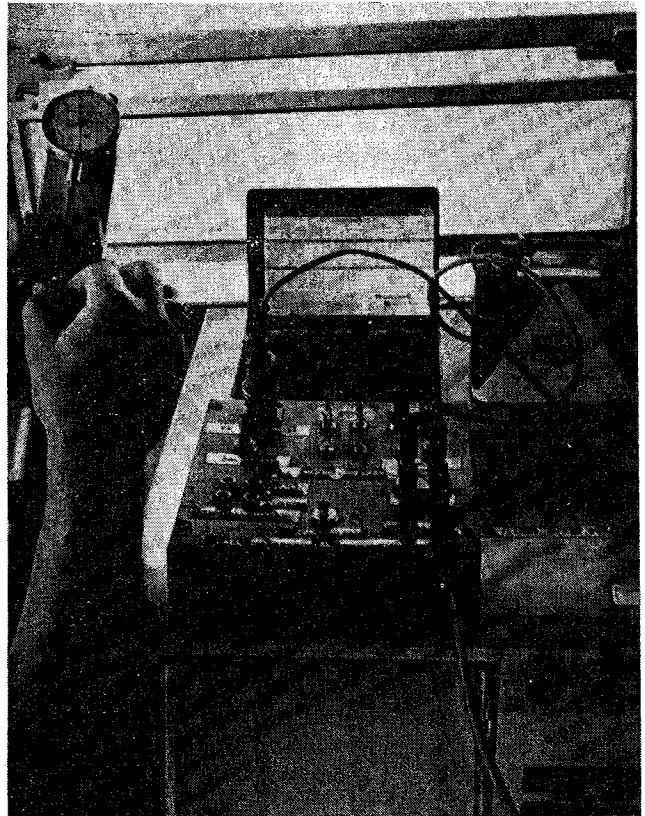
Figure 13. Displacement transducer calibration.
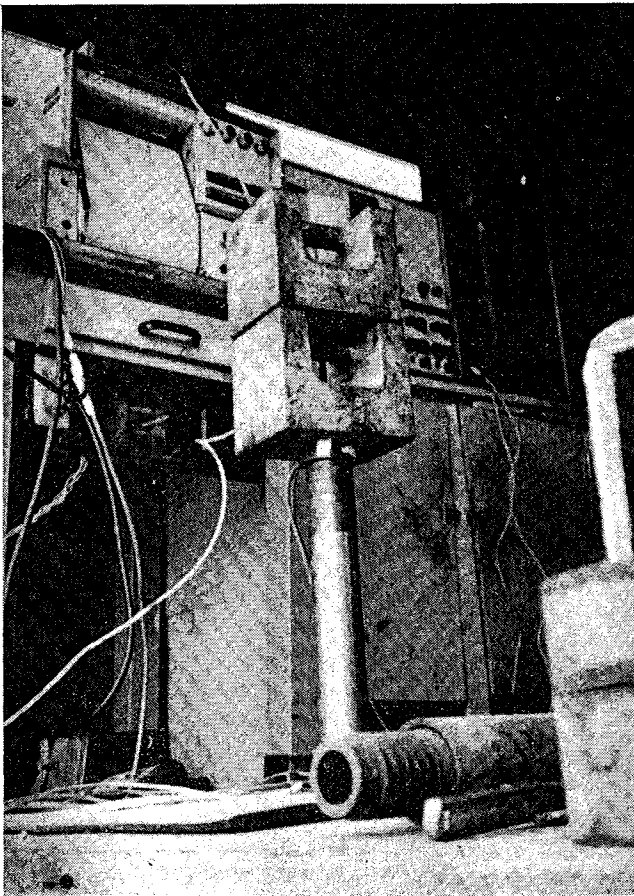
Figure 12. Load cell calibration for dynamic testing.
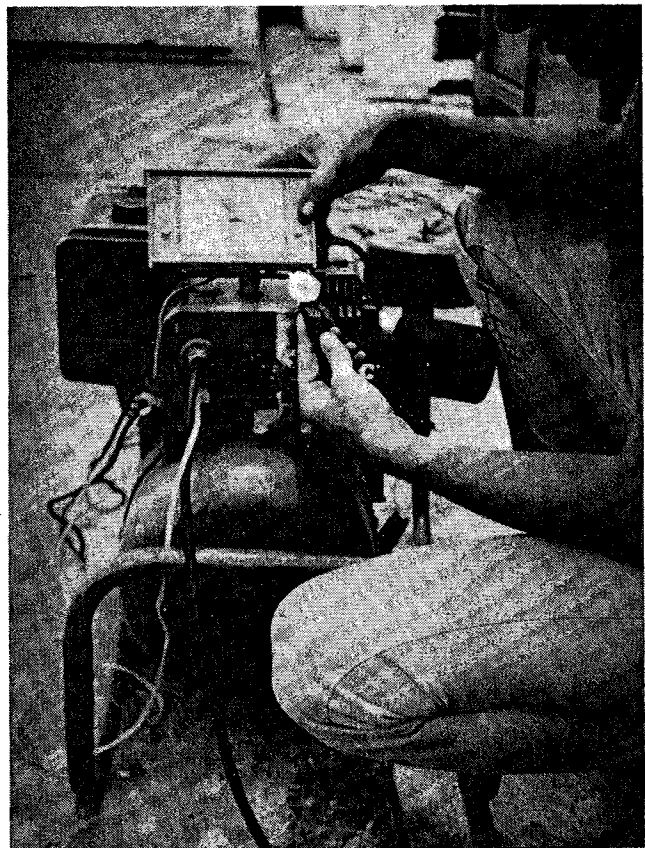
Figure 14. Generator calibration.

that particular weight was noted. This gave a calibration factor for that load cell at a specific gain (see Figure 12).

Before a static test the Budd P-350 strain indicator was balanced at full sensitivity with a load cell other than those being used for the test, it was then unplugged. Initial readings were then taken, before loading, of the bridges to be tested. This procedure was used because a switch and balance strain indicator unit was not available. During testing, the difference between initial reading and test reading was the strain in the cell under a particular load.

Preceding a dynamic test, it was only necessary to balance the bridges, plug in the external calibration resistance, set the desired gain, remove resistance and the system was ready to test.

The linear displacement transducer was calibrated using an Ames dial indicator and moving the magnetic core a known distance (see Figure 13). The resulting deflection of the galvanometer could be adjusted, using a variable resistance calibration unit, to a desired displacement scale.

The power for the recording equipment was supplied by a 2.5-kilowatt gasoline powered generator. To insure that fluctuations in the generator operating frequency did not cause varying test results, it was calibrated. This was accomplished by checking time on a clock connected to the generator with a watch. When both completed a specified period of time at the same instant, the generator was operating at 60 cycles per second. The generator could be slowed down or speeded up by throttle adjustments (see Figure 14).

Chapter III

SOIL PROPERTIES

Boring Log

In regard to a proper test site, initial thoughts were to find an area with a relatively homogeneous soil, preferably clay, to a depth of 10 ft. This would reduce some of the variables involved in the analysis of data.

Preliminary site investigations were run utilizing a Texas Highway Department, District 17, sampling rig. A number of sites throughout the University properties were observed. A site which most closely fit the criteria was found at the Texas A&M Research Annex. It is located at the south end of the third runway.

The site was decided upon at the test area and a boring log was made by the Texas Highway Department, District 17 lab, during early January, 1969 (see Figure 15).

Soil Properties

It was decided that discrepancies which might arise in test data could result from changes in soil properties between different areas or periods of time. In order to document these changes, samples were taken immediately following every test. The soil parameters which were determined from the samples were:

1. Liquid limit,
2. Plastic limit,
3. Natural moisture content,
4. Unconfined compressive strength, and
5. Total unit weight.

Table 1 shows the results of the soil test conducted in connection with each field test. Notice should be taken to the fact that, in most cases, the moisture content at the time of the shear test are less than the natural moisture contents. The probable reason for this is the fact that the samples were tested in the lab several weeks after sampling.

DEPTH (FT.)	SOIL SYMBOL	SAMPLE	DESCRIPTION OF STRATUM	UNIT WEIGHT LBS./CU. FT.	PLASTIC LIMIT	LIQUID LIMIT	MOISTURE CONTENT, %	UNCONFINED SHEAR STR. (PSI)
2			DARK CLAY FIRM TO STIFF	124.4	20	49	25.4	16.4
4			DARK CLAY, FIRM TO STIFF		19	48	27.0	
6			DARK GRAYISH CLAY, FAIRLY STIFF	124.7	21	56	23.6	28.9
8			RED SANDY CLAY, WITH SOME CALCAREOUS NODULES		19	56	24.0	
10			RED SANDY CLAY WITH SOME CALCAREOUS NODULES	125.3	21	65	21.0	58.3

LEGEND		
TYPE OF SAMPLE		SOIL SYMBOL
PUSH BARREL		DARK CLAY
AUGER		RED SANDY CLAY

Figure 15. Boring log.

TABLE I
ENGINEERING PROPERTIES OF TEST SOILS

Date	Site & Test No., etc.	Depth	w_l	w_p	w_n	w_{shear}	Unconfined shear strength (psf)	γ_T (lbs/cf)
4/22	I-1-1	0'-8"		NO DATA OBTAINED				
4/23		2'	53.7	22.6			1095	123.7
4/23		4'	58.5	23.2	22.0		3170	123.3
4/23	I-1-2	6'	63.8	29.8	25.5	25.0	1915	122.1
4/23		8'	66.6	21.6	22.0		4370	124.6
4/26	I-2-1							
4/26	I-2-2	2'-8"	60.8	21.9	25.4	23.1	1478	123.0
4/26	I-2-3							
4/26	I-2-4	5'-4"	61.5	19.5	25.7		1968	127.0
4/30	I-3-1							
4/30	I-3-2	2'-8"	62.6	22.1	24.7		1348	123.8
4/30	I-3-3							
4/30	I-3-4	5'-4"	68.8	24.2	25.9		1952	127.7
5/14	I-4-1							
5/14	I-4-2	2'-8"	53.5	23.8	24.1	23.1	2063	127.9
5/14	I-4-3							
5/14	I-4-4	5'-4"	62.5	28.1	21.9	21.9	2145	128.3
		2'			21.7	21.6	1935	128.3
		4'	58.5	17.6	24.1	22.7	1481	127.3
6/3	II-1-1	6'	65.5	19.1	25.6	23.1	1845	127.3
		8'	60.3	17.6	19.2		5660	132.0
6/11	II-2-1							
6/11	II-2-2	2'-8"	65.5	16.2	24.1	23.1	1575	126.5
6/11	II-2-3							
6/11	II-2-4	5'-4"	64.5	21.1	24.6	23.6	2223	126.5
6/12	II-3-1							
6/12	II-3-2	2'-8"	62.3	23.0	26.0	23.9	2060	127.5
6/12	II-3-3							
6/12	II-3-4	5'-4"	63.7	22.3	24.5	24.3	2970	131.2
6/13	II-4-1							
6/13	II-4-2	2'-8"	55.7	24.6	25.4	24.7	1585	123.9
6/13	II-4-3							
6/13	II-4-4	5'-4"	63.5	19.2	24.3		2900	129.7

Weather Conditions

It should be noted that changes in soil shear strength could be due in large part to changes in weather over extended periods of time. At the time of the original THD soil boring in January, the weather was cold and no excessive moisture was noticed. The first test series was run over a period of several weeks. The initial three tests of the first test series were performed during a period of greater-than-average rainfall. The last test of series I was run during a drying out period which subsequently became a prolonged period of extreme heat and dryness. It was during this period that test series II was performed.

Chapter IV

TEST PROCEDURES

Introduction

Basically a test series consisted of static tests and dynamic tests. The static tests were performed on the 8-ft drill pipe, simultaneous device and configurations of the tip-only and skin friction devices. Dynamic tests were performed only on the simultaneous device. An outline of static and dynamic test procedures is given initially and is followed by a more detailed discussion of a complete test series.

Static Test Procedure

The following procedure was used during static tests:

1. The horizontal reaction member was inserted in the load frame.

2. The Budd P-350 strain indicator was balanced using a cell other than the one to be tested.

3. An initial reading was taken on the Budd P-350 strain indicator of the cells to be used during the test.

4. The linear displacement transducer was calibrated and attached to the drill pipe.
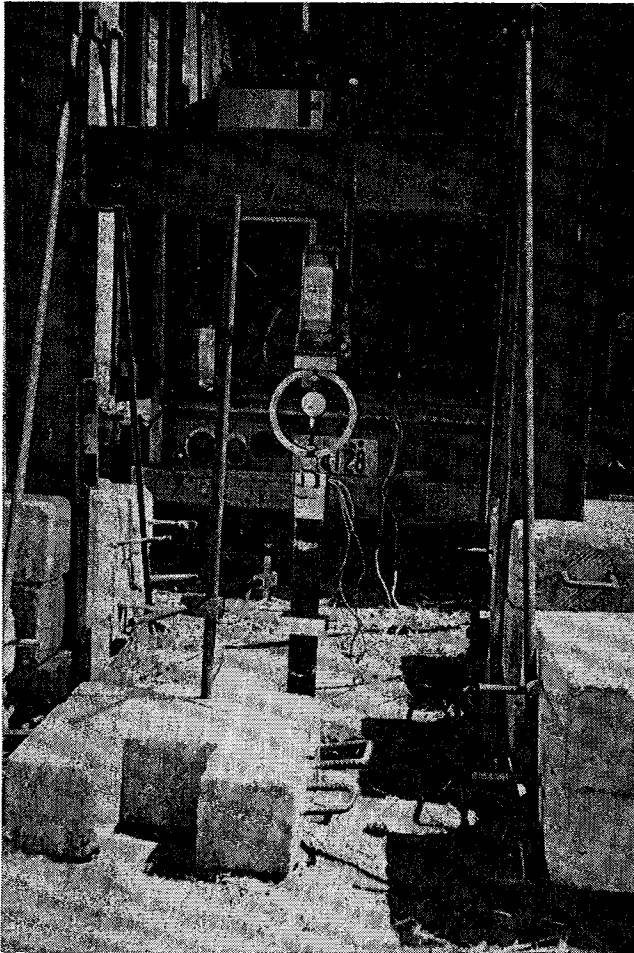
5. The jack and proving ring were put atop the pipe.

6. Loads were then applied to the pile in 2½ min. increments. On the 8-ft drill pipe, loads were applied at the rate of 500 lb per 2½ min. The other devices were loaded at a rate of 100 lb per 2½ min. The loads were applied and readings monitored on the Budd P-350 strain indicator until failure occurred (see Figure 16 for the static test set-up).

Dynamic Test Procedure

The following procedure was used during dynamic tests:

1. Using the amplifier and visicorder, the bridges were balanced and the gain set for a convenient scale.

2. The linear displacement transducer was calibrated and attached to the drill pipe.

3. The weight was then dropped upon the drill pipe at heights of 3 in., 6 in., and 9 in. (see Figure 17 for dynamic set-up).
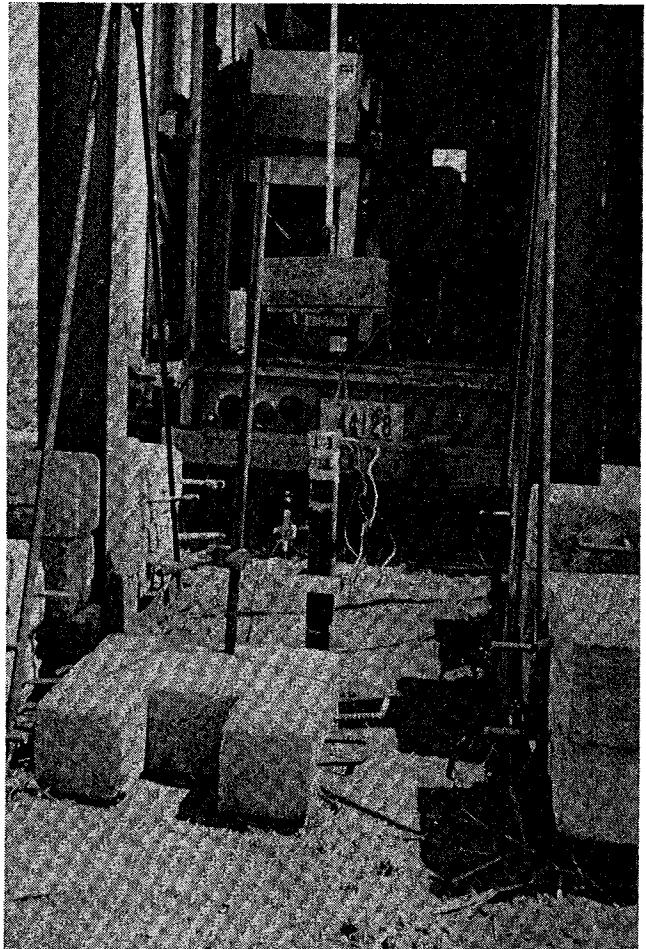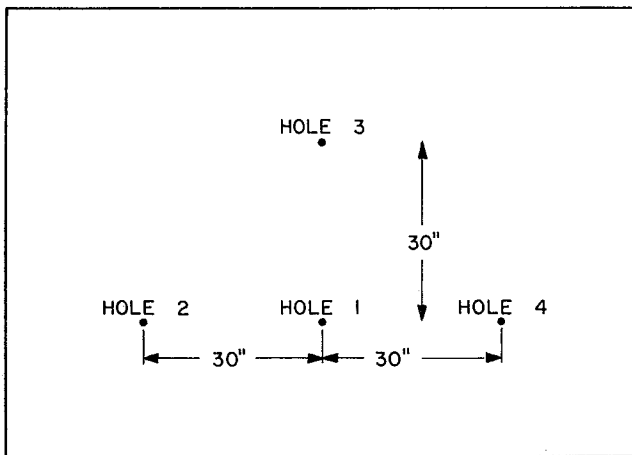

Figure 16. Static test setup.

Figure 17. Dynamic test setup.

HOLE 1: TEST OF 8 FT. INSTRUMENTED DRILL PIPE

HOLE 2: TESTS WITH SIMULTANEOUS DEVICE

HOLE 3: TESTS WITH SKIN FRICTION DEVICE AT TOP

HOLE 4: TESTS WITH SKIN FRICTION AND TIP ONLY DEVICES TOGETHER

Figure 18. Layout of test area.

Test Series

Each test series involved a number of tests conducted in four test holes. For identification purposes, tests on a specific device were designated as a "hole." This designation yields:

Hole 1: Test on a 8-ft section of Instrumented Drill Pipe

Hole 2: Tests utilizing the Simultaneous Device

Hole 3: Tests utilizing the Skin Friction Cell at the top of the drill pipe.

Hole 4: Tests utilizing the Tip-Only and Skin Friction Device used together.

The approximate layout of a test area is shown in Figure 18.

The 8-ft section of drill pipe was driven using the load frame and standard penetration tripod. After it was driven to an embedded length of 8 ft, a static test was performed. Figure 19 shows the approximate location of the devices during testing. The pile was then removed from the ground.

The simultaneous device was then tested. Prior to testing, a hole was hand-augered to the depth of 2 ft-8 in., a drill pipe attached to the cell and the device inserted in the hole. The device was then jacked 10 in. into the ground and a static test run. Upon completion of the static test, dynamic tests were run. The device was then removed from the ground. The hole was then further augered to a depth of 5 ft-4 in. and the above procedure repeated (see Fig. 20).

Tests at hole 3 consisted of utilizing the skin friction load cell at the top of the drill pipe (see Fig. 21). Initially the hole was augered to a depth of 2 ft-8 in. The drill pipe with load cell at the top was then inserted in the hole with only the tip resting on the hole bottom.
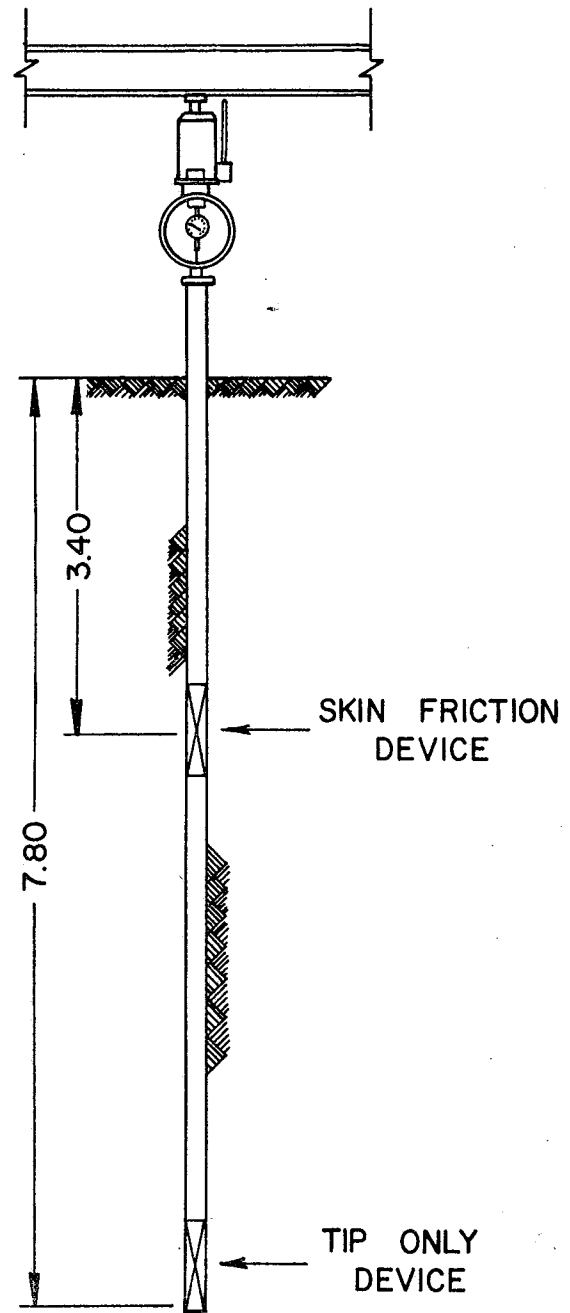

Figure 19. Eight-foot pile test.

A static test was then run. The pipe was then jacked 10 in. into the ground and tested statically. The pipe was removed from the ground. The hole was then augered to a depth of 5 ft-4 in. and the above procedure repeated.

Tests at hole 4 consisted of using the tip-only and skin friction cells together as shown in Fig. 22. A hole was hand augered to a 2 ft-8 in. depth, drill pipe attached to the cell and the device inserted in the hole. Initially, the device rested only on the hole bottom and a static test was run. The cell was then jacked 15 in. into the ground and another static test run. The device was then removed from the ground, the hole augered to 5 ft-4 in. and the procedure repeated.
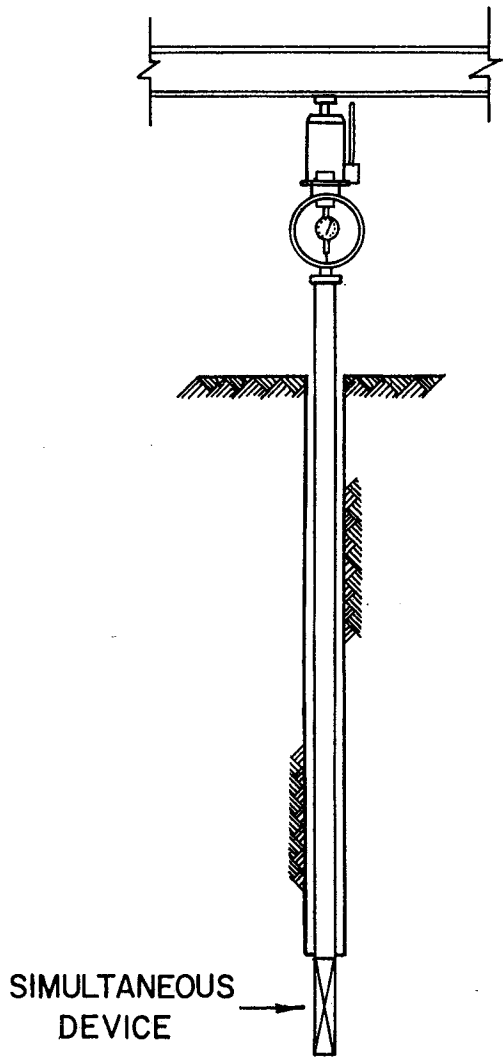
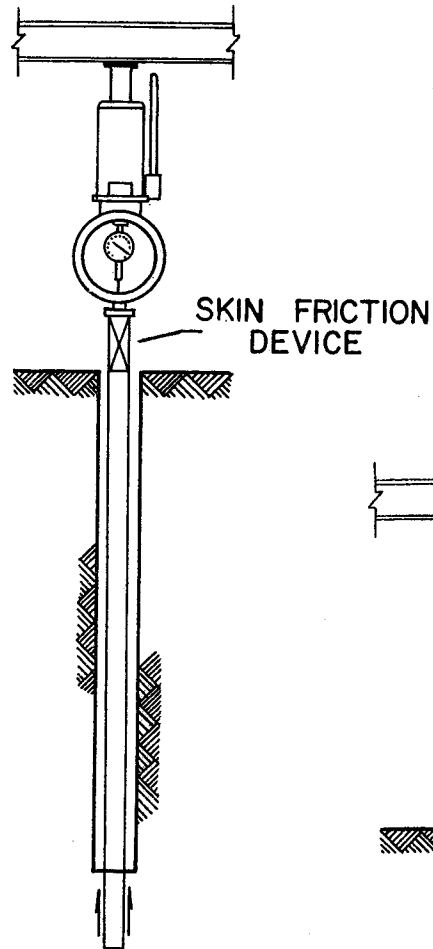Figure 20. *Test with simultaneous device.*

SIMULTANEOUS DEVICE

SKIN FRICTION DEVICE

Figure 21. *Test with load cell at top.*

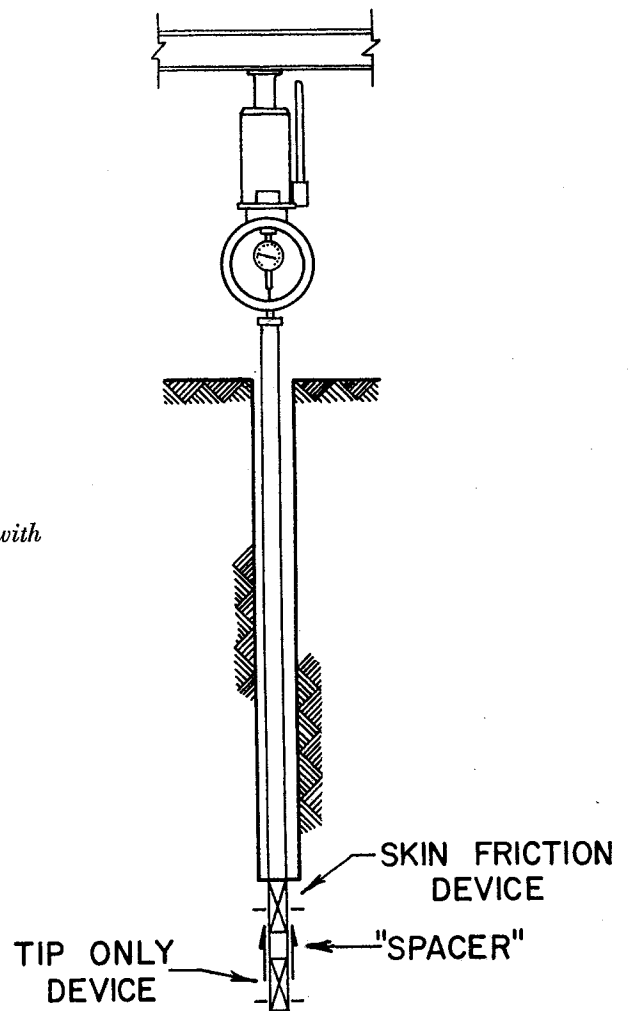SKIN FRICTION DEVICE

"SPACER"

TIP ONLY DEVICE

Figure 22. *Test with load cells together.*

Chapter V

ANALYSIS OF STATIC TESTS

Test Designation

A total of three series of tests were run at the same site. Designation and description of each test is shown in Table II.

Data Reduction

In reducing the data, it was thought that in order to compare values, the limiting value of skin friction would be an important common factor for the different devices. Point bearing values could also be compared.

The procedures for calculating these values for the different devices are discussed in this section.

The 8-ft pile gave load readings at 3.40 ft and 7.80 ft from the surface (see Fig. 19). It was decided to obtain skin friction values between the load cells and compare these to values of skin friction obtained from the devices at similar depths. This value was obtained by taking the load carried in a segment and dividing by the circumferential area. Note Figure C-3, Appendix C, for an example calculation. The point bearing value could be obtained by dividing the tip load by the tip area.

TABLE II
TEST DESIGNATION AND DESCRIPTION

Series	Hole	Test	Depth	Description of Test
I	1	1	0'-8'	Test no good
I	1	2	0'-8'	8 ft pile tested statically to failure
I	2	1	2'-8"	Test no good
I	2	2	2'-8"	Simultaneous device tested dynamically
I	2	3	5'-4"	Simultaneous device tested statically to failure
I	2	4	5'-4"	Simultaneous device tested dynamically
I	3	1	2'-8"	Load cell at top, tip-only static test to failure
I	3	2	2'-8"	Load cell at top, 10 in embedded static test to failure
I	3	3	5'-4"	Load cell at top, tip-only static test to failure
I	3	4	5'-4"	Load cell at top, 10 in embedded static test to failure
I	4	1	2'-8"	Load cells together, tip-only static test to failure
I	4	2	2'-8"	Load cells together, 15 in embedded static test to failure
I	4	3	5'-4"	Test no good
I	4	4	5'-4"	Test no good
II	1	1	0'-8"	8 ft pile tested statically to failure
II	2	1	2'-8"	Simultaneous device tested statically to failure
II	2	2	2'-8"	Simultaneous device tested dynamically
II	2	3	5'-4"	Simultaneous device tested statically to failure
II	2	4	5'-4"	Simultaneous device tested dynamically
II	3	1	2'-8"	Load cell at top, tip-only static test to failure
II	3	2	2'-8"	Load cell at top, 10 in embedded static test to failure
II	3	3	5'-4"	Load cell at top, tip-only static test to failure
II	3	4	5'-4"	Load cell at top, 10 in embedded static test to failure
II	4	1	2'-8"	Load cells together, tip-only static test to failure
II	4	2	2'-8"	Load cells together, 15 in embedded static test to failure
II	4	3	5'-4"	Load cells together, tip-only static test to failure
II	4	4	5'-4"	Load cells together, 15 in embedded static test to failure
III	1	1	12"	Simultaneous device tip only test—plunging failure*
III	1	2	12"-24"	Simultaneous device—total load, tip load, skin friction measurement. Embedded 1' in ground—plunging failure*
III	1	3	24"	Two load cells together. Tip only test—plunging failure*
III	1	4	24"-36"	Two load cells together. Total load, tip load, skin friction measurement. Embedded 1' in ground—plunging failure*
III	2	1	12"	Simultaneous device tip only test—plunging failure**
III	2	2	12"-24"	Simultaneous device—total load, tip load, skin friction measurement. Embedded 1' in ground—plunging failure**
III	2	3	24"	Two load cells together. Tip only test—plunging failure**
III	2	4	24"-36"	Two load cells together. Total load, tip load, skin friction measurement. Embedded 1' in ground—plunging failure**
III	3	1	12"-48"	Load cell at top, two load cells together. All load cells monitored as pile was embedded into ground at constant rate of 3" per minute to depth of 4 feet
III	4	1	12"-48"	Load cell at top, two load cells toether. All load cells monitored as pile was embedded into ground at constant rate of 3" per minute to depth of 4 feet
III	5	1	12"-48"	Load cell at top, simultaneous device. Continuous monitoring as pile was embedded into ground at constant rate of 3" per minute to depth of 4 feet

*Plunging failure attained by Texas Highway Department drill rig using hydraulic system.
**Plunging failure attained by jacking to failure.

The simultaneous device gave a tip load and a skin friction load over a 7.5-in. length (note Figure 23). The skin friction was obtained by dividing this value by the circumferential area of 7.5-in. length. Unit tip load was computed by dividing the tip load by the tip area.

In order to compute a skin friction value for the load cell at the top test, the failure load of the tip-only test was subtracted from the 10 in. embedded test failure load and divided by the circumferential area. This gave an estimated skin friction. In other words, it is assumed that the tip load would remain the same, irregardless of any interaction between skin friction and tip load. Data from test series III shows that this assumption is not correct.

The skin friction for the load cells together device was calculated in much the same manner as the simultaneous device. The tip cell load was subtracted from the top cell load and divided by the circumferential area of the distance between the bridges. Unit tip load was calculated by dividing tip load by tip area.

Load Versus Movement Curves

For each static test, load versus movement curves were plotted (see Appendix A). This gave the following curves for the stated tests:

Simultaneous Device

    1. Point bearing versus movement curve.

    2. Skin friction versus movement curve.

Load Cell at Top

    1. Point bearing versus movement curve.

    2. Total load versus movement curve.

    3. Estimated skin friction versus movement curve.

Load Cells Together

    1. Point bearing versus movement curve.
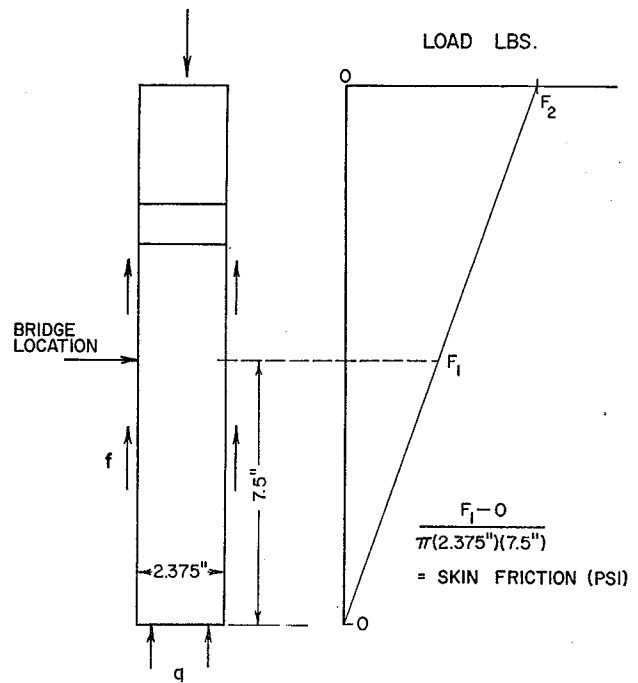
    2. Skin Friction versus movement curve.

Figure 23. Load distribution assumption for simultaneous device.

Limiting values of skin friction and point bearing were obtained from the curves. Although only limiting values were obtained, in every case the entire curve was plotted so that anyone interested in load versus movement relationships could find the information in this report. Load versus settlement and load distribution curves were also plotted for the 8-ft pile tests (see Appendix C).

Test Series I

A tabulation of test results and shear strength data for series I is found in Table III.

TABLE III
TEST SERIES I RESULTS

Date	Device Type	Test No.	Depth	Device Limiting Values (psf)	8 ft Pile Limiting Values (psf)	Unconfined Shear Strength (psf)
4/23	8 ft Pile	I-1-2	0'-3.40'		205	1095
			3.40'-7.80'		952	1915
4/26	Simultaneous	I-2-1	2'-8"		TEST NO GOOD	
4/26		I-2-2	2'-8"		DYNAMIC TEST	
4/26		I-2-3	5'-4"	Tip = 1880 Friction = 1572	952	1968
4/26		I-2-4	5'-4"		DYNAMIC TEST	
4/30	Load Cell at Top	I-3-1	2'-8"	Tip = 2110 Friction = 1276	205	1348
4/30		I-3-2	2'-8"			
4/30		I-3-3	5'-4"	Tip = 3600		
4/30		I-3-4	5'-4"	Friction = 2710	952	1952
5/14	Load Cells Together	I-4-1	2'-8"	Tip = 2730 Tip = 3250		
5/14		I-4-2	2'-8"	Friction = 1309	205	2063
5/14		I-4-3	5'-4"		TEST NO GOOD	
5/14		I-4-4	5'-4"		TEST NO GOOD	

The limiting value of skin friction for the upper 3.40 ft of the 8-foot pile (Test I-1-2) is very low (205 psf). It was observed during driving of the section that a small gap extended to some unknown depth around the test pile at the ground surface. It was judged that this was possibly caused by repeated jarring of the soil during driving. It was also thought that overburden pressures would cause closure of the gap at greater depths. Therefore, it would seem that the upper skin friction values should not be considered as being a representative value. The average skin friction value for the lower part of the 8-ft pile was found to be 952 psf. This compared to values of 1572 psf and 2710 psf obtained from the devices in Tests I-2-3 and I-3-4, respectively. These values do not compare favorably and there seems to be little correlation either between the devices or with the 8-foot instrumented section.

An attempt was made to explain the lack of correlation by studying the changes in soil shear strength in the different test holes. It should be noted at this point that unconfined compression tests were not run immediately following sampling. Samples were wrapped and waxed when taken and stored in a moisture room. It was found that the moisture contents for the unconfined compression test samples were not the same as the moisture contents for the in-situ samples. Table I, Chapter III shows the changes noted in the moisture contents. Some of the shear test moisture contents in series I are absent due to loss of moisture cans in the drying oven. Because of the changes in moisture, which in turn resulted in shear strength changes, it was felt that soil shear strength could not be used to explain differences in the in-situ measurements.

Tests I-4-1 and I-4-2 indicate that point bearing values increased when the device was embedded 15 inches. This is shown due to the fact that Test I-4-1 was a tip-only test at the bottom of the hole and Test I-4-2 was an embedded test with both skin friction and point bearing measurements.

Tests I-1-1, I-2-1, I-4-3, and I-4-4 were no good due to instrumentation difficulties which occurred after the tests started.

Test Series II

A tabulation of test results and shear strength data for series II can be found in Table IV.

For the reason that has been stated in the previous section, the skin friction value of 132 psf over the top 3.40 feet of the 8-foot pile is questionable.

The lower part of the 8-foot pile had an average skin friction value of 1670 psf. Test II-2-3 had a friction value of 1805 psf, which is a percent error of 8.08%. Test II-3-4 showed a friction value of 1770 psf which yields a percent error of 5.98%. Test II-4-4 had a friction value of 2490 psf giving a percent error of 49.1%. Shear strength values could not be used to explain the lack of correlation of Test II-4-4 as the shear strength for Test II-3-4 is essentially the same as for Test II-4-4 yet a large difference shows up in skin friction values. It is possible that these shear strength values are not correct because of changes in moisture content which occurred between sampling and testing as discussed previously.

Tests II-4-1, II-4-2, and tests II-4-3 and II-4-4 indicate also that point bearing is greater in an embedded test as compared to a tip-only test. Test II-4-3, a tip-only test, gives a point bearing value of 4460 psf whereas Test II-4-4, an embedded test, gives a point bearing value of 10,000 psf. Such a large increase does not seem possible unless the tip in the later test was situated in a soil strata with a much higher shear strength.

As a result of the apparent lack of correlation of the data from test series I and II, it was decided that a change in test procedures should be made and a third series of tests should be conducted. Instead of trying to correlate limiting values of skin friction in different test holes, it was felt that emphasis should be placed on comparing the changes in frictional resistance resulting from changes in tip load and soil shear strength in one test hole. Any changes should correlate with changes in soil shear strength if the shear strength determinations are made immediately after field testing.

TABLE IV
TEST SERIES II RESULTS

Date	Device Type	Test No.	Depth	Device Limiting Values (psf)	8 ft Pile Limiting Values (psf)	Unconfined Shear Strength (psf)
6/3	8 ft Pile	II-1-1	0'-3.40'	.	132	1935
			3.40'-7.80'		1670	1845
6/11	Simultaneous	II-2-1	2'-8"	Tip = 2059 Friction = 1145	132	1575
		II-2-2	2'-8"		DYNAMIC TEST	
		II-2-3	5'-4"	Tip = 2910 Friction = 1805	1670	2223
		II-2-4	5'-4"		DYNAMIC TEST	
6/12	Load Cell at Top	II-3-1	2'-8"	Tip = 2730		
		II-3-2	2'-8"	Friction = 1345	132	2060
		II-3-3	5'-4"	Tip = 3600		
		II-3-4	5'-4"	Friction = 1770	1670	2970
6/13	Load Cells	II-4-1	2'-8"	Tip = 2760		
		II-4-2	2'-8"	Tip = 3025 Friction = 1735	132	1585
	Together	II-4-3	5'-4"	Tip = 4460		
		II-4-4	5'-4"	Tip = 10,000 Friction = 2490	1670	2900

TABLE V
TOTAL SURFACE LOAD REDUCTION FACTOR

Series	Hole	Test	Total Surface Load Tip Only Test (lbs.)	Total Surface Load Embedded Test (lbs.)	Tip Load Embedded Test (lbs.)	Percent Reduction in Tip Load (%)
III	1	1	1460			
		2		3500	685	$\frac{685}{1460}$ (100) = 47.0
		3	1750			
		4		4050	1020	$\frac{1020}{1750}$ (100) = 58.3
III	2	1	2250			
		2		5420	1240	$\frac{1240}{2250}$ (100) = 55.0
		3	1500			
		4		3700	940	$\frac{940}{1500}$ (100) = 62.6

Average Reduction Factor = 55.7%

Test Series III

A tabulation of test data for series III is shown in Table V and VI and the data for test III-3-1 are plotted in Figure 24. Before discussing these data, the main procedural differences between this series and series I and II should be discussed briefly.

The main problem encountered in series I and II was the variation in soil properties and the questionable accuracy of the shear strength determinations. To overcome these problems the five tests included in series III were conducted in holes only 1 foot apart, depths of penetration were between 12 inches and 48 inches, and at least 6 soil samples were taken in each hole and tested for shear strength immediately.

A detailed description of each series III test conducted in the five test holes is given in Table II. For each test a load cell was used at the ground surface in order to monitor total surface load for both the tip only tests and the embedded tests. This procedure was followed so that total surface load and tip load could be related through a reduction factor. Determination of a reduction factor would allow all load measurements to be made at the surface and greatly simplify the test procedure in the field.

Tip load only tests were conducted at 12-inch depths in holes 1 and 2 with the simultaneous device and at 24-inch depths with the two-load-cell device. Both devices were embedded one foot in holes 1 and 2 and allowed

TABLE VI
FRICTION DATA

Series	Hole	Test	Total Surface Load Tip Only Test T_L — (lbs)	Embedded Test Total Load T_B — (lbs)	Embedded Test Tip Load T_T — (lbs)	Measured Friction* F_M — (Psf)	Computed Friction** F_C — (Psf)
III	1	1	1460				
		2		3500	685	4550	4320
		3	1750				
		4		4050	1020	4870	4940
III	2	1	2250				
		2		5420	1240	6730	6675
		3	1500				
		4		3700	940	4430	4620
III	3	1	1525				
				1790	850	1510	1512
III	4	1	2140				
				3060	1910	3140	3010
III	5	1	3600				
				4460	2060	3860	3960

Measured Friction* $F_M = \dfrac{T_B - T_T}{A***}$ A***: Contact area $= \dfrac{(\pi)\ (2.375)\ (12)}{144} = .621$ sq. ft.

Computed Friction ** $F_C = \dfrac{(T_B) - (T_L)\ (.557)}{A***}$

to stand for 15 minutes before plunging failure tests were conducted. In all cases plunging failure was assured by forcing a movement of at least one inch. The devices in hole 1 were loaded slowly and continuously with the hydraulic equipment on the drilling rig. The devices in hole 2 were loaded with a hydraulic jack using 500-pound load increments with each load held for 2½ minutes. The devices in holes 3, 4, and 5 were pushed at a constant rate of approximately 3 inches per minute from a depth of 12 inches to a depth of 48 inches. Total surface loads, friction loads, and tip loads were monitored continuously during these continuous loading tests.

The pertinent data from the tests conducted in holes 1 and 2 which were used to evaluate the reduction factor are shown in Table V. In all cases the tip load measured after the device was embedded one foot, was less than the tip load which equaled the total surface load in the tip-only test. Determination of the percent reduction in tip load is shown in Table V and the average reduction factor for this soil is 55.7%. It *was* noted that the total loads in the tip-only test and the tip loads in the embedded tests increased or decreased in each test in direct relationship to increases or decreases in the soil shear strength. This relationship is shown clearly in Figure 24. It would be possible for the tip load to increase significantly as it did in tests II-4-3 and II-4-4 if the soil became very stiff within the one foot of embedded length. It was determined that tests I-4-1, I-4-2, II-4-1, and II-4-2, were in error because the tip-only tests were not carried to plunging failure, and consequently the tip-only values are too low. The tip-only values in tests I-4-1 and II-4-1 were obtained for a movement of only 0.1 inches and a movement of at least 1.0 inches was required in the series III tests in order to get an ultimate tip value.

The reduction factor of 55.7% as determined in Table V was used to compute a friction value for all five test holes and the computed friction values were compared with measured friction values. These data are shown in Table VI. The correlation between computed friction using the reduction factor and the measured friction using the in-situ devices is very good, especially
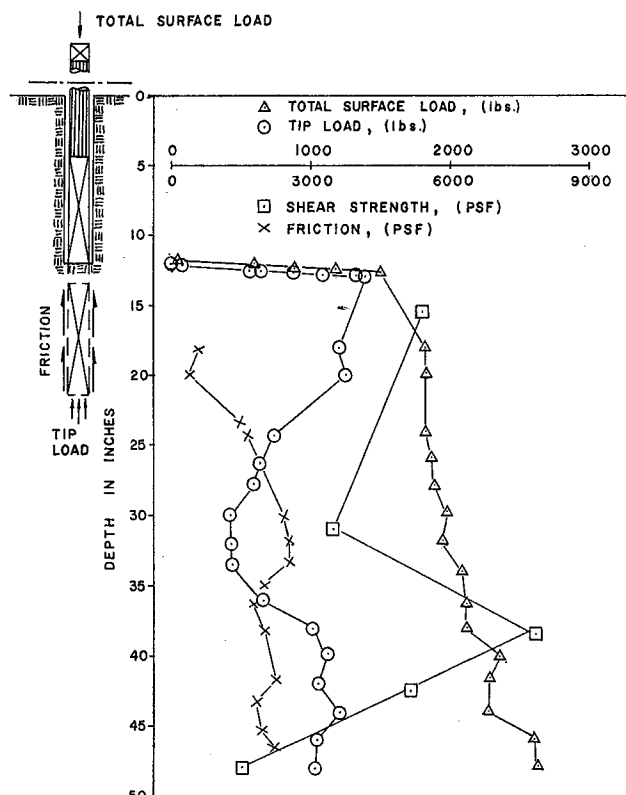
Figure 24. Data from Test III-3-1.

for Tests III-3-1, III-4-1, and III-5-1. These data were taken from the 12-inch to 24-inch penetration for each test. The significance of the correlation is that once a reduction factor is obtained it is possible to determine friction values by making measurements only at the surface. This permits a much simpler test procedure. The data shown in Figure 24 are for the continuous penetration test III-3-1. It should be noted that the tip load changes with the soil shear strength and friction values change in relation to changes in the tip load.

Chapter VI

ANALYSIS OF DYNAMIC TESTS

Background

Many problems dealing with piling behavior have been studied in recent years using a dynamic approach. Smith (8) formulated such an approach using transmission of stress waves through the pile as the foundation of his method.

Smith used an idealized pile-soil system in which the pile and other equipment used on the pile during driving are treated as lumped masses and springs. The soil action was represented by springs, sliding blocks and dashpots (see Figure 25). The springs and sliding blocks represent the elastic and plastic properties of the

soil and the dashpot, a viscous damping property. A formula he used to describe resistance to driving is:

$$P_{dynamic} = P_{static} (1 + J\dot{x}) \qquad (2)$$

where $P_{dynamic}$ = maximum dynamic resistance,

P_{static} = maximum static resistance, and

J = a viscous damping constant used when describing the soil resistance.

$\dot{x}$ = velocity of a pile segment in any time interval. Smith assumed load-deformation curves, both static
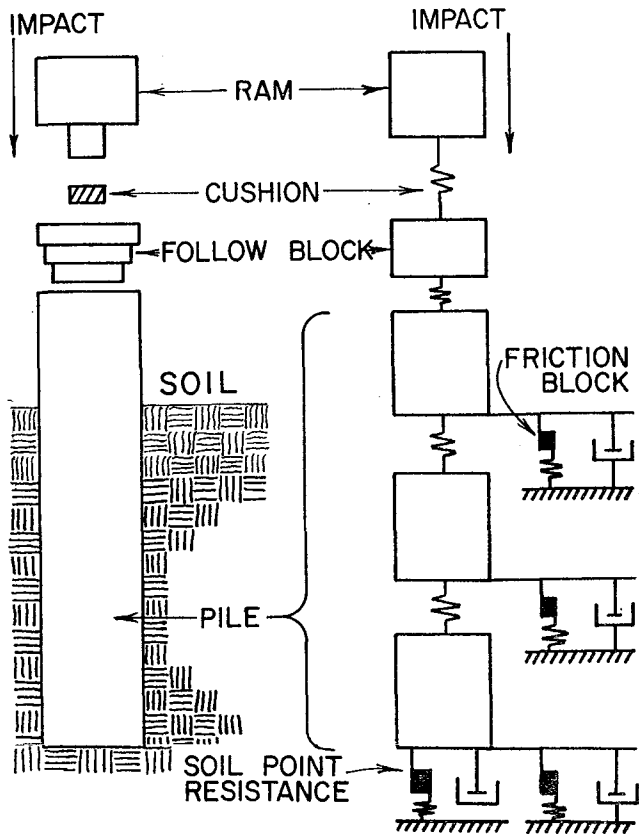
Figure 25. *Smith's model.*

Figure 26. *Soil load-deformation assumption.*

and dynamic, for soils (see Figure 26). Under static loading, soil resistance for a certain deformation (x) is:

$$P = Kx$$

Under dynamic loading, the increase in load due to dashpot action is:

$$P_a = c\dot{x}$$

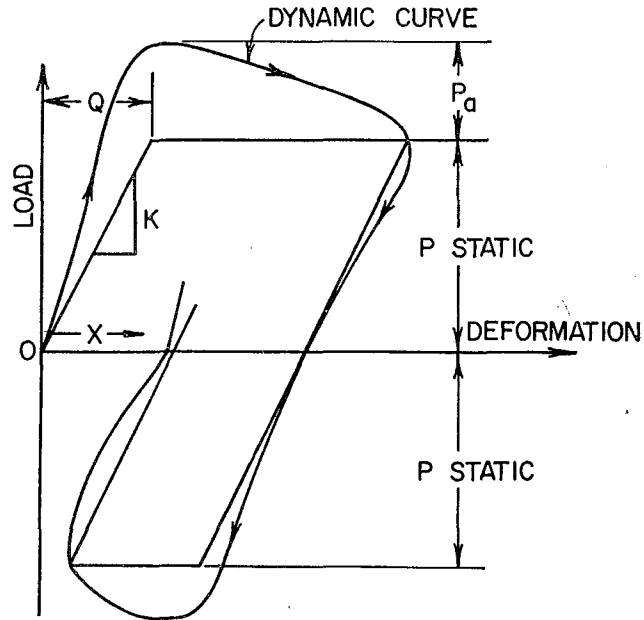where P_a = additional soil resistance due to dynamic load,

c = a viscous damping constant, and

$\dot{x}$ = velocity of soil deformation (fps).

The total resistance becomes the static plus the additional due to dynamic load, or:

$$P_{dynamic} = Kx + c\dot{x}$$

Smith (8) then used:

$$c = Kx(J) \quad or \quad c = Kx(J')$$

Depending on whether the damping in question was tip (J) or friction (J'). Since Kx has been defined as a static soil resistance, then equation (2) can be written as follows:

$$P_{dynamic} = P_{static} (1 + (J \text{ or } J')\dot{x}) \qquad (3)$$

TABLE VII
TIP DAMPING DATA

Site & Hole	Depth	Height of Drop	P_{dy} (lbs)	P_{st} (lbs)	P_{dy}/P_{st}	Pile Displacement Velocity (fps)	J (sec/ft)
I-2	2'-8"	3"	470	272	1.73	3.19	.229
I-2	2'-8"	6"	587	272	2.16	3.66	.317
I-2	2'-8"	9"	760	272	2.79	5.14	.349
I-2	5'-4"	3"	712	220	3.23	2.78	.803
I-2	5'-4"	6"	740	220	3.36	3.26	.724
I-2	5'-4"	9"	740	220	3.36	4.44	.532
II-2	2'-8"	3"	391	240	1.63	2.44	.259
II-2	2'-8"	6"	522	240	2.17	5.02	.233
II-2	2'-8"	9"	740	240	3.08	5.26	.396
II-2	5'-4"	3"	608	340	1.79	2.34	.337
II-2	5'-4"	6" (#1)	804	340	2.36	3.74	.364
II-2	5'-4"	6" (#2)	740	340	2.18	3.71	.318
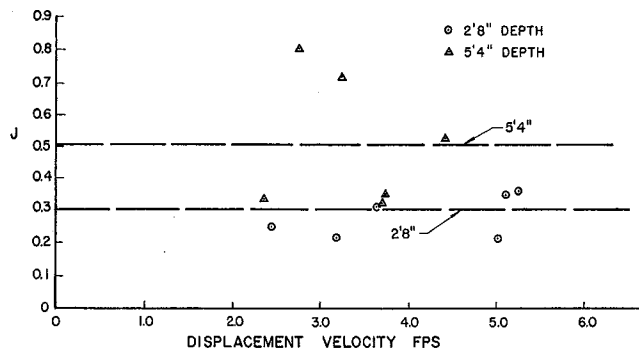
Figure 27. Tip damping constant vs pile displacement velocity.

Figure 28. Friction damping constant vs pile displacement velocity.

Data Reduction

The viscous damping constants J and J′ were the unknowns in the analysis. They were calculated from equation (3) as follows:

$$J = \frac{\dfrac{P_{dynamic}\ (tip)}{P_{static}\ (tip)} - 1}{\overset{\cdot}{x}}$$

and

$$J' = \frac{\dfrac{P_{dynamic}\ (friction)}{P_{static}\ (friction)} - 1}{\overset{\cdot}{x}}$$

Table VII shows the values for J obtained from the dynamic tests and Table VIII shows the values obtained for J′.

Figure 27 shows the values of J plotted versus displacement velocity. It was decided that in order to take overburden into account somehow, that an average J would be calculated for both the 2 ft-8 in. and 5 ft-4 in. depths. Smith recommended a J value of 0.15 for fine grained soils while Korb found a value of 0.18 more suitable. The average J values found in this research were .30 for the 2 ft-8 in. depth and .51 for the 5 ft-5 in. depth as shown in Figure 27.

Figure 28 shows the values of J′ plotted versus displacement velocity and the curve established by Korb.

Figure 29. Friction damping constant vs pile displacement velocity using modified Smith model.

From the plot, it is seen that there is reasonably good correlation, although the data obtained in this study are slightly higher for this range of displacement velocities. No tests were run at smaller velocities. The higher values would seem to indicate that overburden pressures do make a difference in both J and J′ determination. Korb (5) modified equation (3) to give:

$$P_{dynamic} = P_{static}\ (1 + J'\ x^N) \tag{4}$$

By setting N = 0.35 in equation (4) Korb found the J′ values could be made a constant. The constant J′ value he found was 1.25 which compares to a J′ value of 0.85 found in this study (See Fig. 29).

TABLE VIII
FRICTION DAMPING DATA

Site & Hole	Depth	Height of Drop	P_{dy} (lbs)	P_{st} (lbs)	P_{dy}/P_{st}	Pile Displacement Velocity (fps)	J′ (sec/ft)	$J'^{0.35}$
I-2	2′-8″	3″	1396			3.19		
I-2	2′-8″	6″	1540			3.66		
I-2	2′-8″	9″	1610			5.14		
I-2	5′-4″	3″	1930	610	3.16	2.78	.750	.945
I-2	5′-4″	6″	1926	610	3.15	3.26	.659	.864
I-2	5′-4″	9″	1980	610	3.25	4.44	.507	.788
II-2	2′-8″	3″	1560	445	3.51	2.44	.103	1.0104
II-2	2′-8″	6″	1660	445	3.74	5.02	.546	.809
II-2	2′-8″	9″	1760	445	2.94	5.26	.368	.705
II-2	5′-4″	3″	1856	700	2.65	2.34	.704	.885
II-2	5′-4″	6″ (#1)	2180	700	3.12	3.74	.568	.821
II-2	5′-4″	6″ (#2)	2096	700	2.99	3.71	.536	.804

Chapter VII

CONCLUSIONS AND RECOMMENDATIONS

Conclusions

Objectives of the research study consisted of three parts: (1) to design and fabricate several in-situ testing devices, (2) to conduct field tests involving the measurement of in-situ skin friction and point bearing during sampling operations, and (3) to recommend a test procedure and device for use in future field test programs. The first two objectives have been accomplished and the third objective will be accomplished in the recommendations section of this chapter.

This study is considered preliminary in nature because the testing devices and procedures are in the development stage. Therefore, no specific conclusions can be given concerning the application of test results. However, the following general conclusions are made concerning the test devices and the test procedures:

1. In-situ measurements of skin friction and point bearing can be made using either the simultaneous device or the two-load-cells with a spacer. However, the test procedure is complicated because connecting wires must be run through the drill pipe from the strain gages in the testing device to the ground surface.

2. In-situ measurements of skin friction and point bearing can be made using a single load cell on top of the drill pipe at the ground surface. This procedure involves the determination of a reduction factor which is used to compute friction, since only tip load and total embedded load are measured. However, the test procedure is simple since all measurements are made at the ground surface.

3. Dynamic tests can be conducted using the simultaneous device, and damping constants can be determined for friction (J') and tip (J) loading. Only a limited number of dynamic tests were conducted in this study so the results are not conclusive. However, indications are that overburden pressure (depth) does influence the magnitude of these parameters.

Recommendations

As a result of the tests conducted in this study the following procedure is recommended for future in-situ field testing:

1. Using the standard THD drilling rig equipment, advance the test hole to the desired depth.

2. Retract and remove drilling equipment and insert drill pipe with a blunt end to the bottom of the test hole.

3. Connect a load cell at the top of the drill pipe and conduct a tip-only test by measuring the total surface load required to move the drill pipe downward one inch.

4. Push the drill pipe assembly downward one foot so that the pipe in the bottom of the test hole will be embedded 12 inches, and wait five minutes.

5. Conduct an embedded test by measuring the total surface load required to move the drill pipe downward one inch.

6. Remove the load cell at the surface, retract the drill pipe and remove the blunt end, attach drilling equipment, and advance the test hole to the next test depth.

7. Repeat this procedure until measurements are made at any number of desired depths.

It should be noted that a direct measurement of skin friction is not made using this procedure. Skin friction will have to be computed using the method presented in Table VI. However, if in-situ measurements are made at a site where a full-scale instrumented pile is being tested, the adjustment factors (reduction or increase) can be determined using the friction data from the instrumented pile test.

During the analysis of test data for any future test program it would be helpful to have soil shear strength data available. Therefore, it is recommended that soil samples be taken during in-situ testing and shear strength determinations should be made immediately. It has been shown in this report that moisture content changes can occur during long moisture-room storage periods.

References

1. Bauder, E. R., "Thorough Site Study Pays off in Better Bridge Design," *Roads and Streets Magazine,* March, 1963.

2. Bowles, Joseph E., *Foundation Analysis and Design,* McGraw-Hill Book Company, New York, 1968.

3. Chellis, Robert, *Pile Foundations,* McGraw-Hill Book Company, New York, 1951.

4. Foundation Exploration and Design Manual, Texas Highway Department, Bridge Division, January 1964.

5. Korb, Kenneth W., Unpublished Thesis, Texas A&M University, January 1969.

6. "Miniature Pile Drivers Pre-Determine Pile Lengths," *Railway Engineering and Maintenance Magazine,* October, 1949.

7. Schmertmann, John H., "Static Cone Penetrometers for Soil Exploration," Civil Engineering ASCE, June, 1967.

8. Smith, E. A. L., "Pile-Driving Analysis by the Wave Equation," *Journal of the Soil Mechanics and Foundations Division,* Proceedings of the American Society of Civil Engineers, Vol. 86, No. SM4, pp. 35-61, 1960.

Appendix A

STATIC LOAD-DEFORMATION CURVES
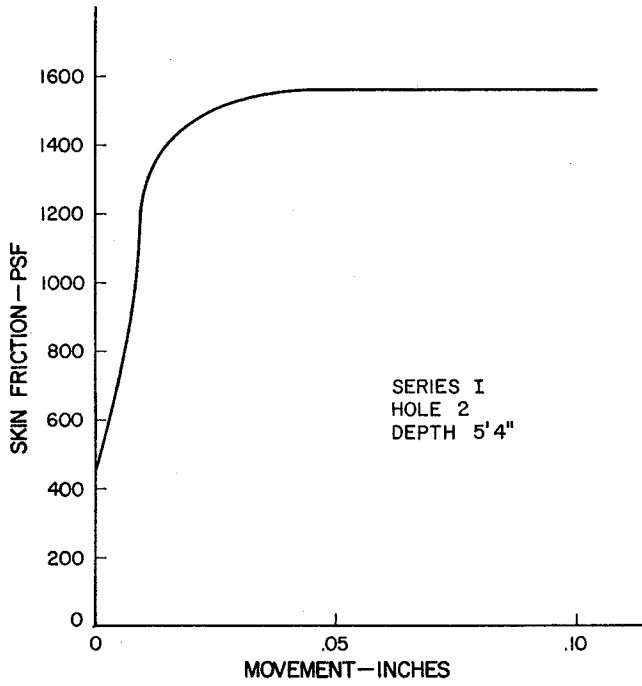
Figure A-1. Skin friction vs movement curve.
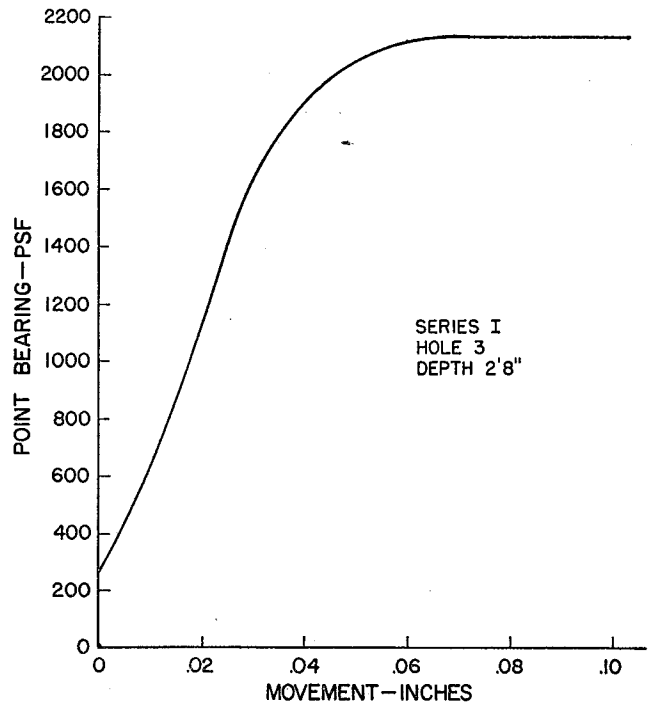
Figure A-3. Point bearing vs movement curve.
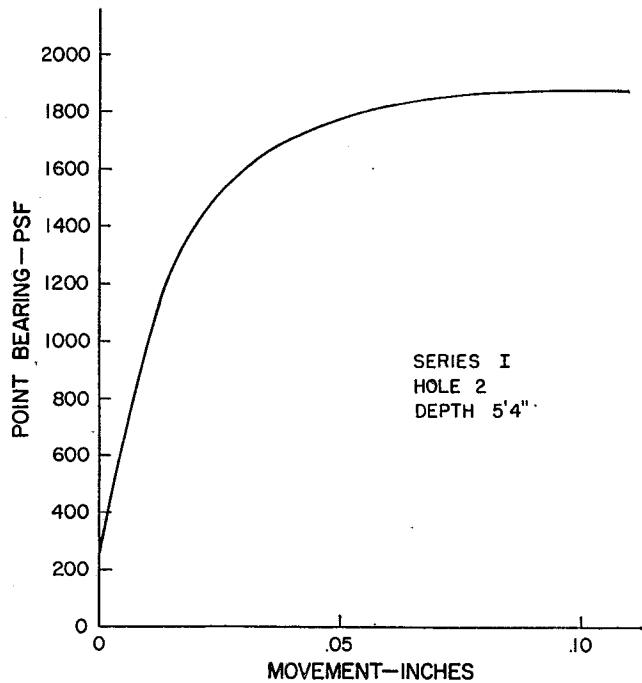
Figure A-2. Point bearing vs movement curve.
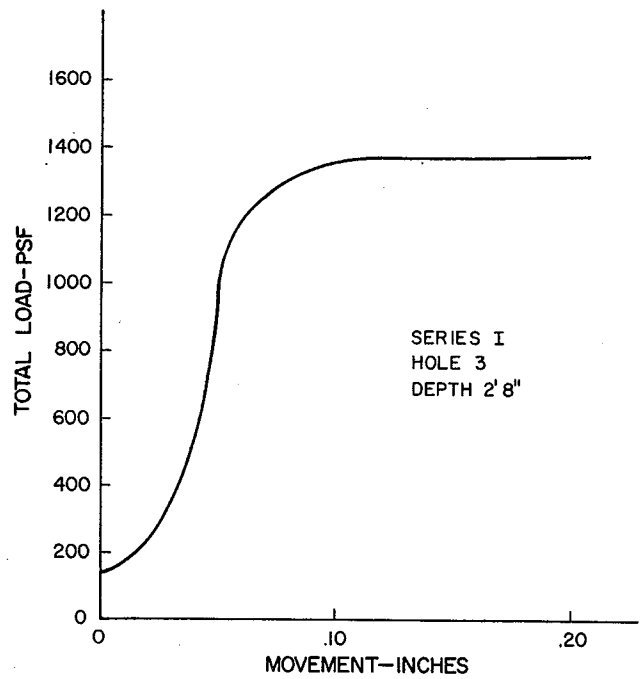
Figure A-4. Total load vs movement curve.
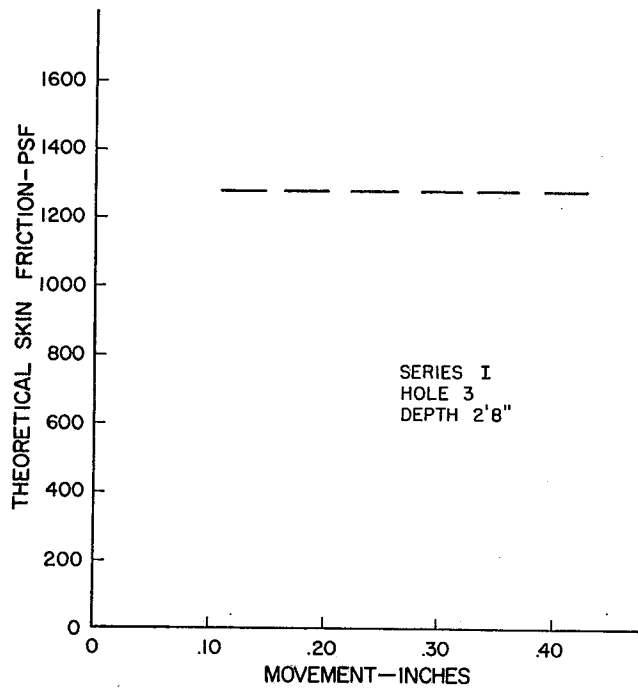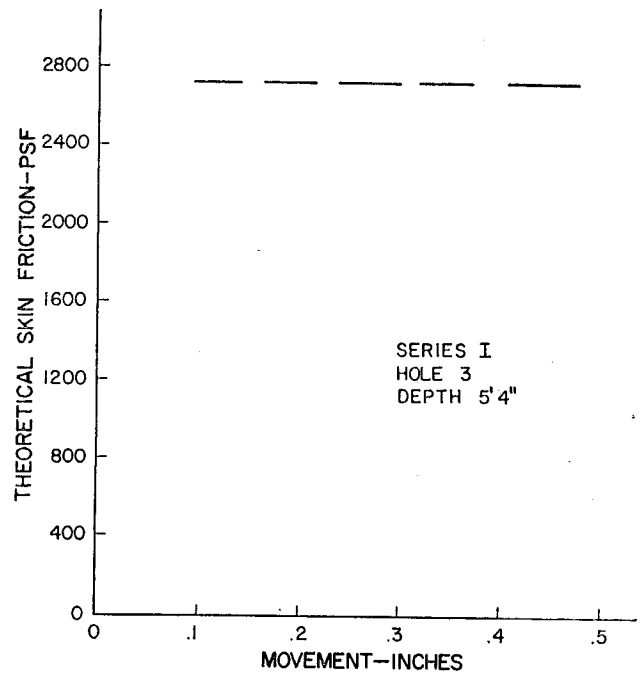
Figure A-5. *Theoretical skin friction vs movement curve.*

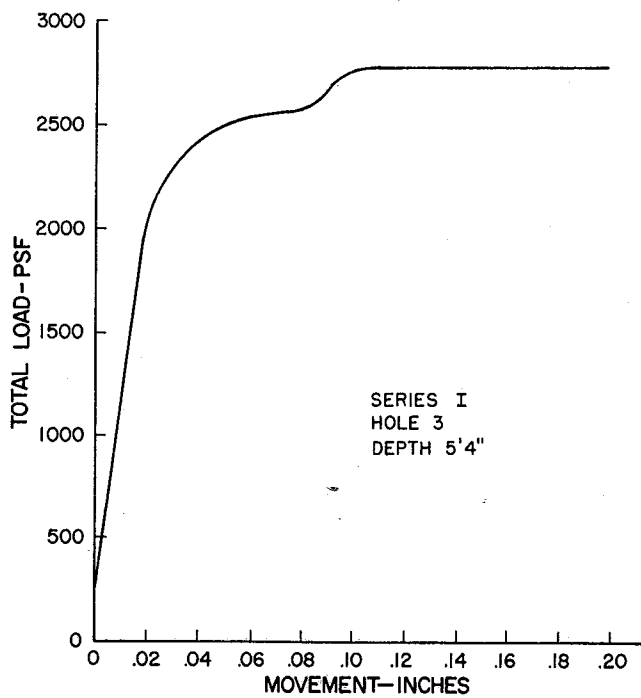Figure A-7. *Theoretical skin friction vs movement curve.*
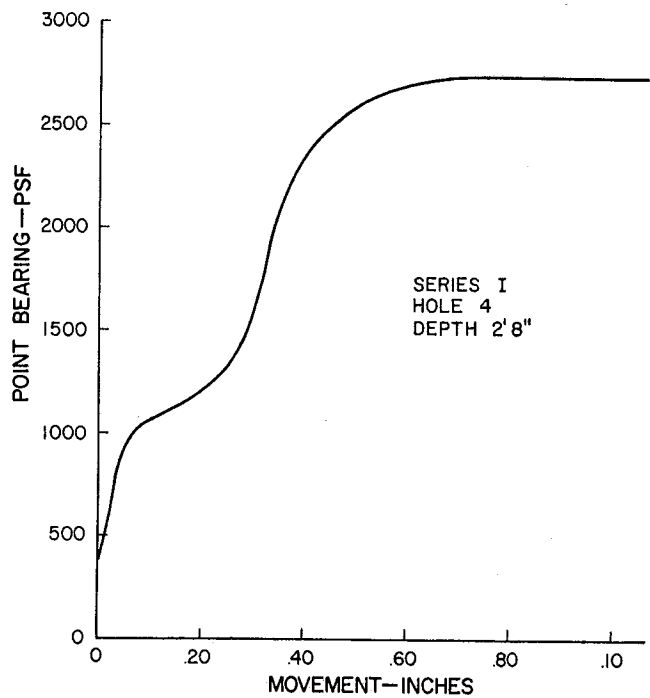

Figure A-6. *Total load vs movement curve.*
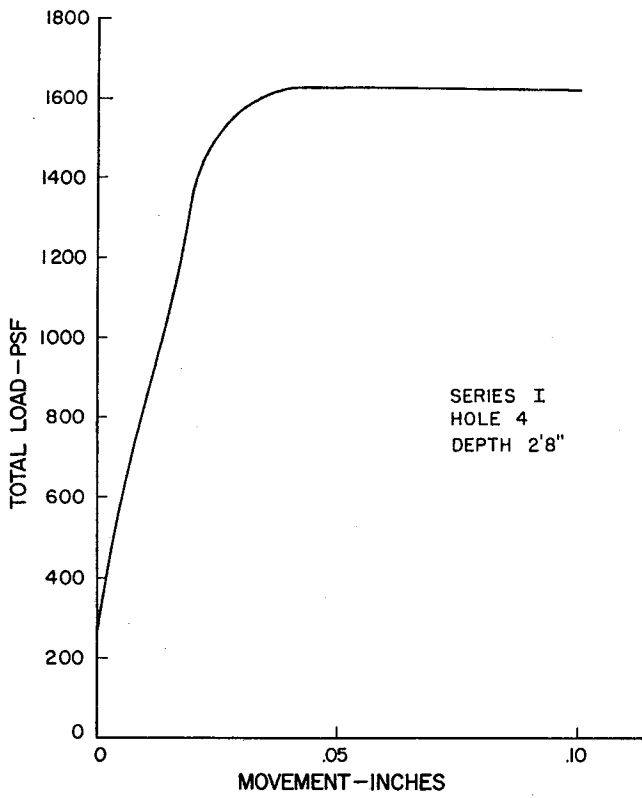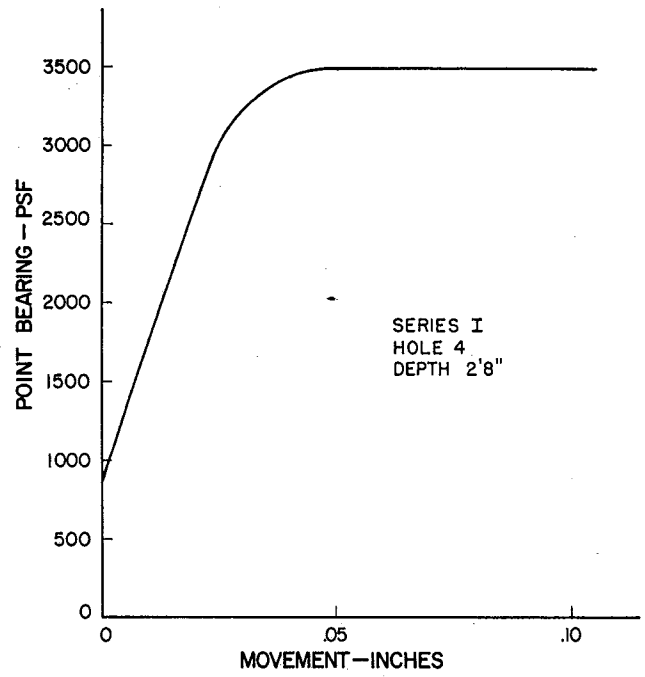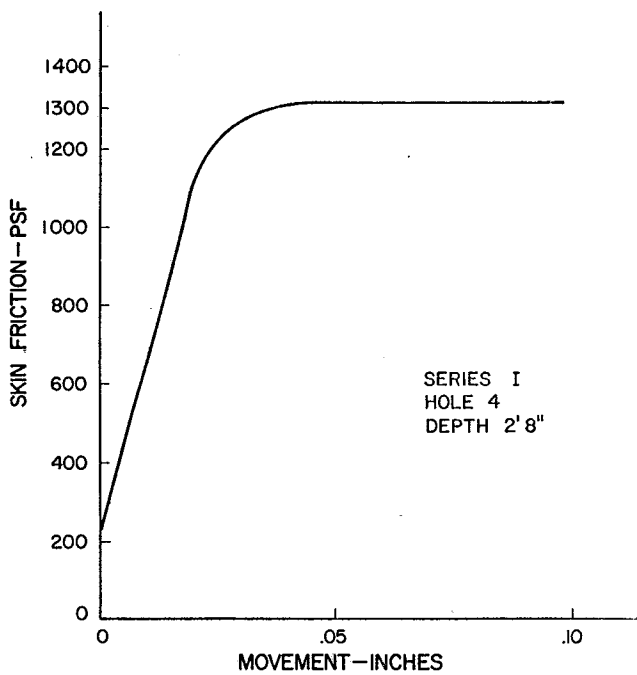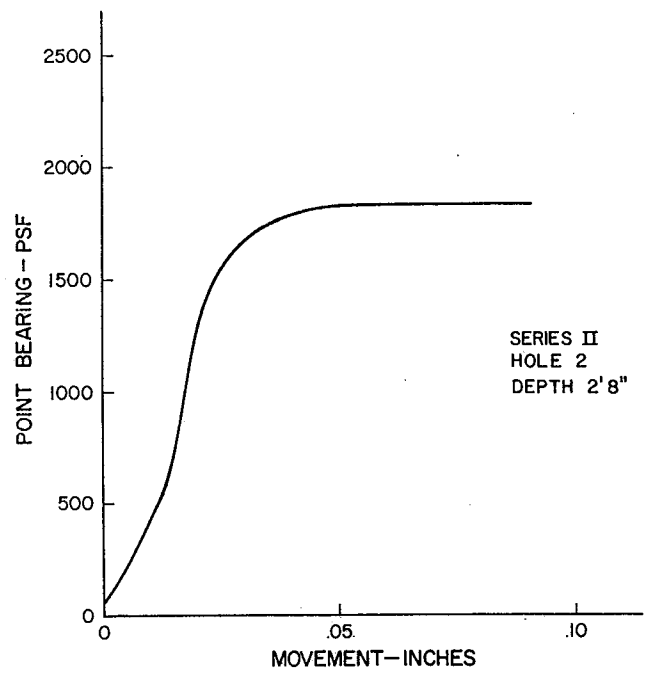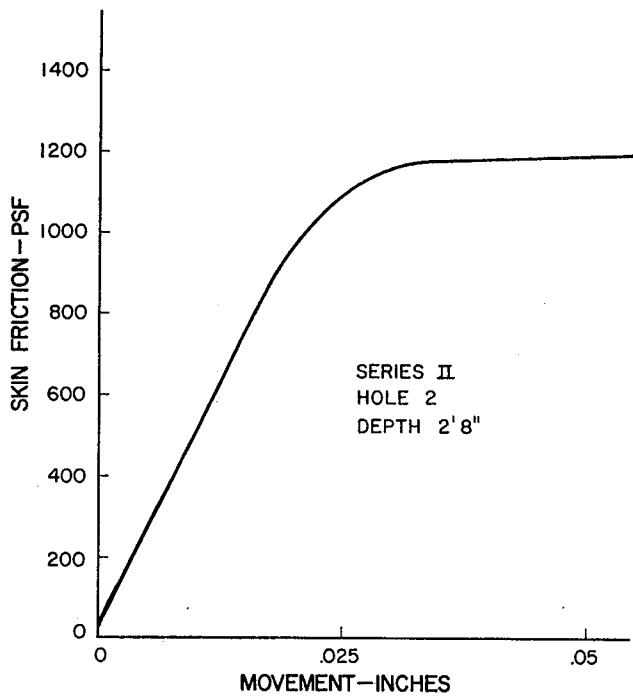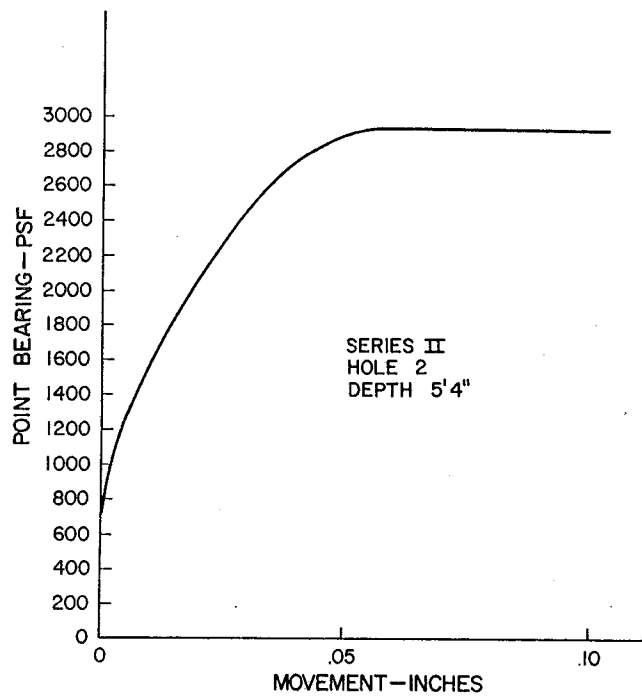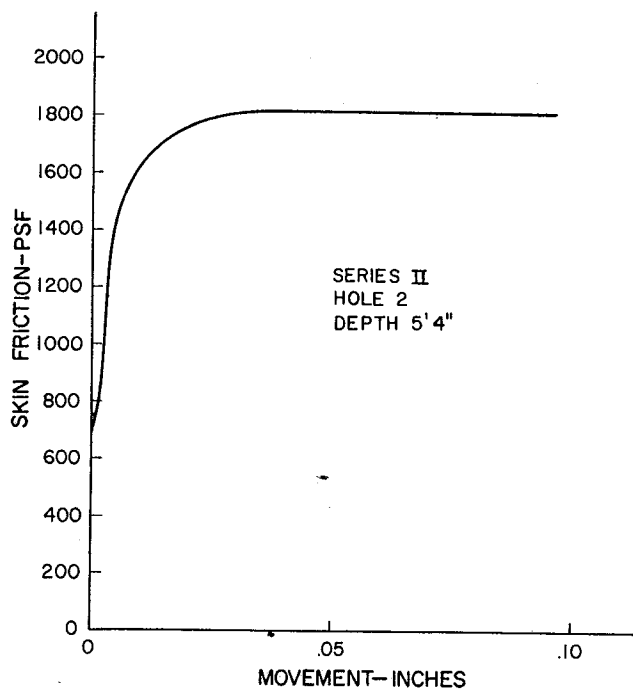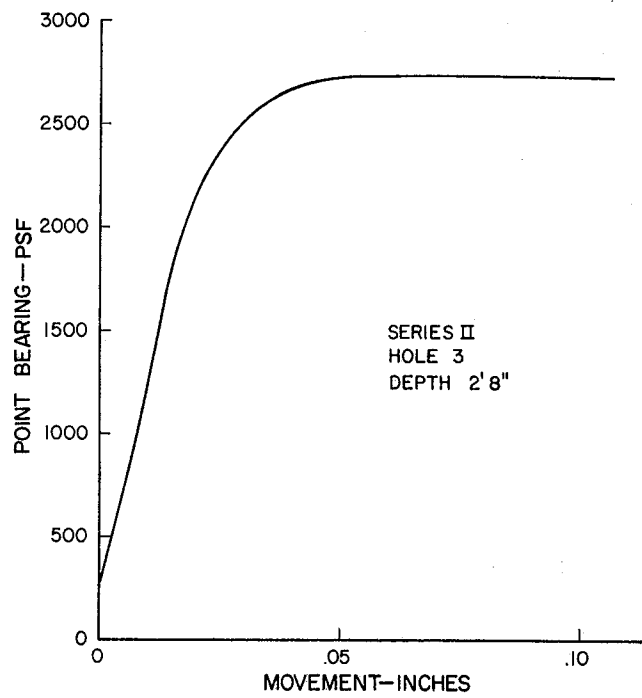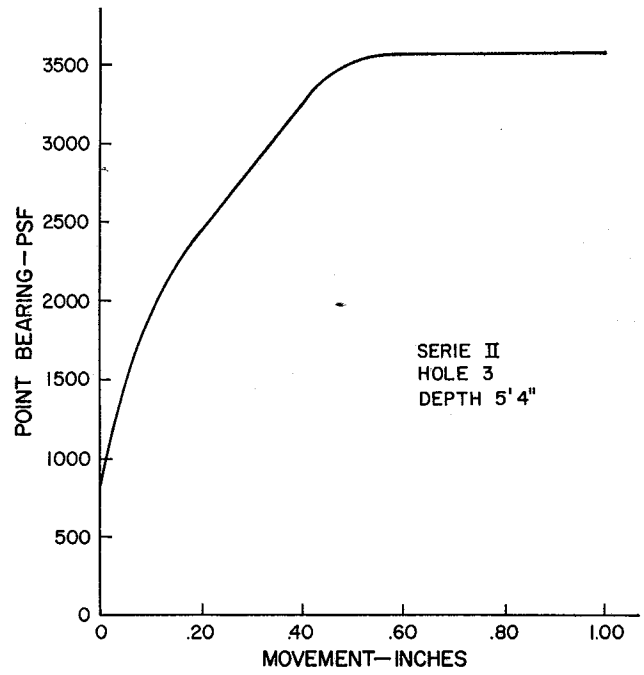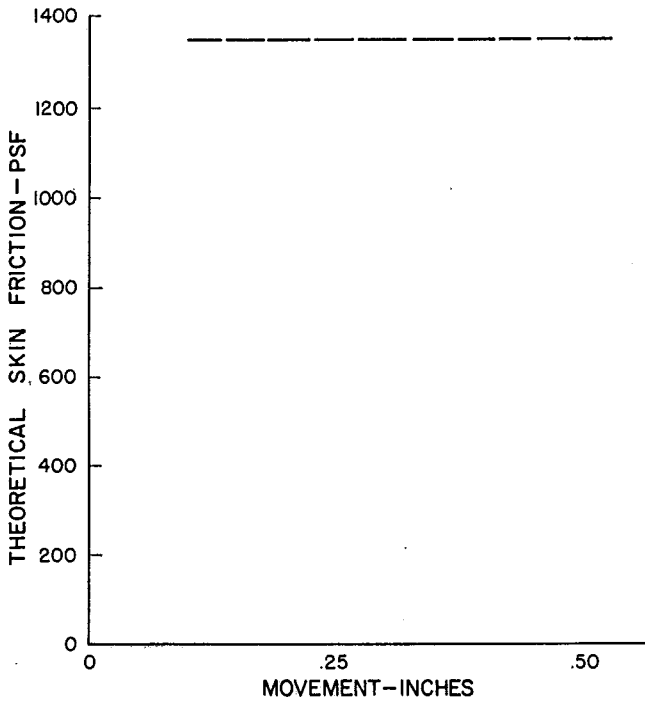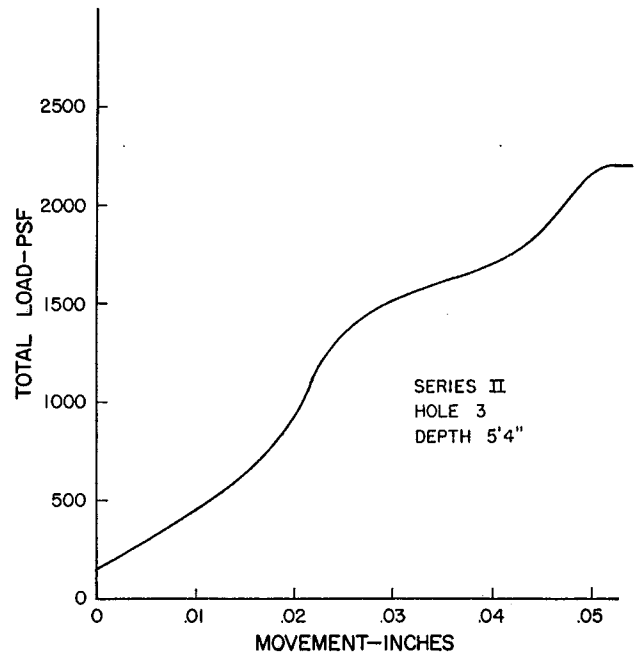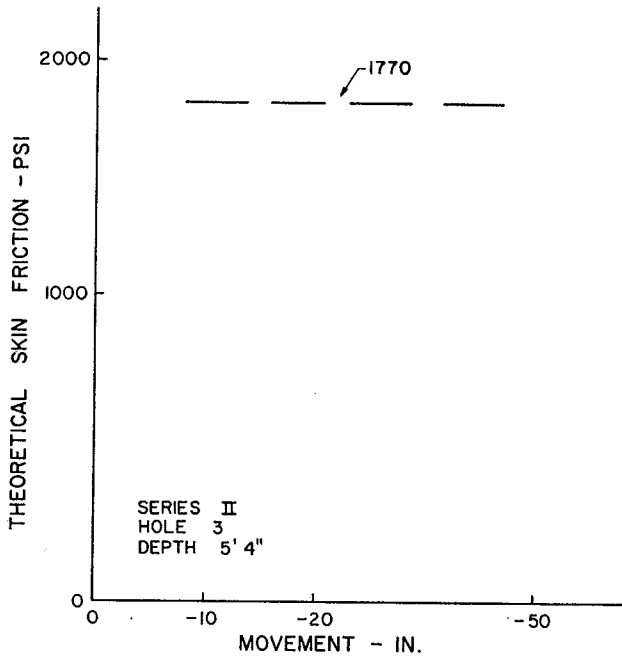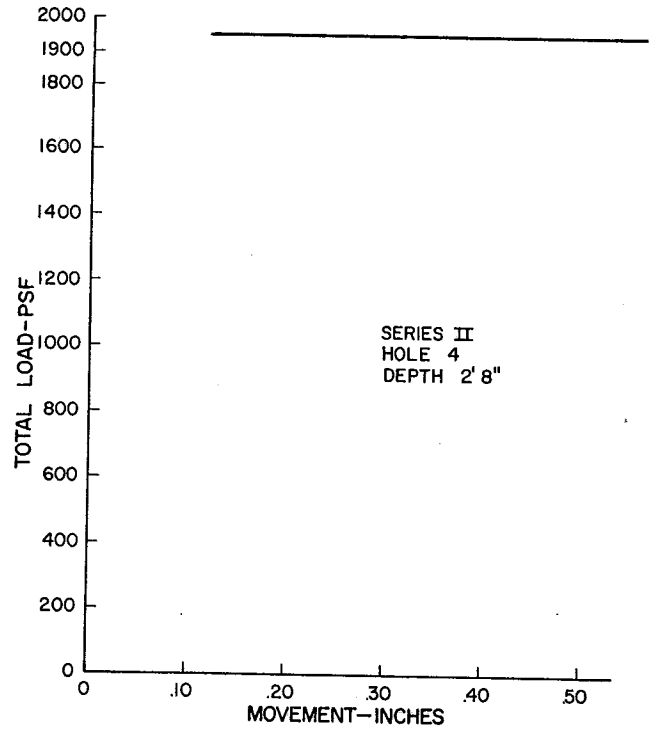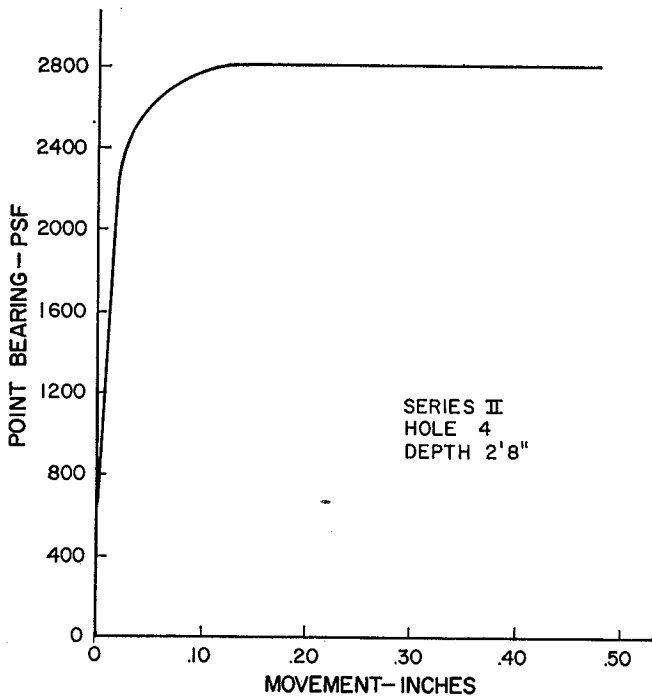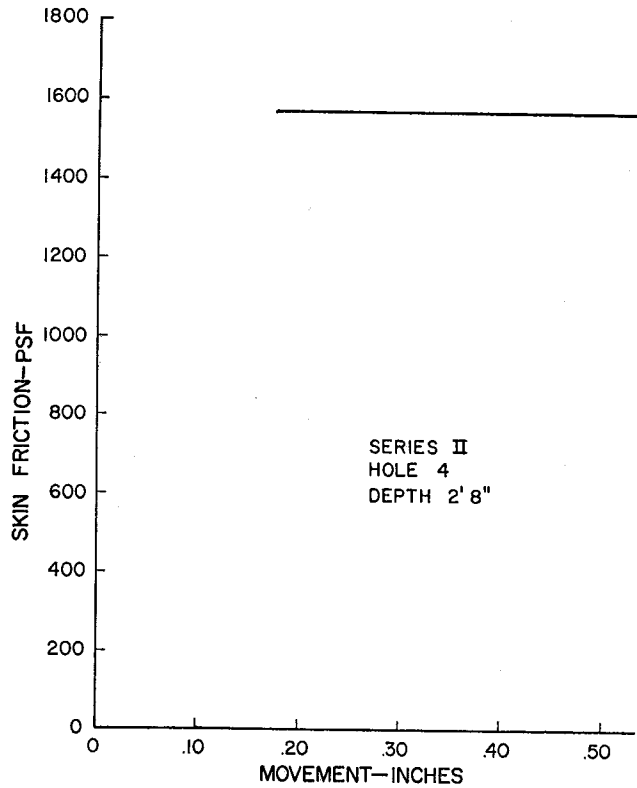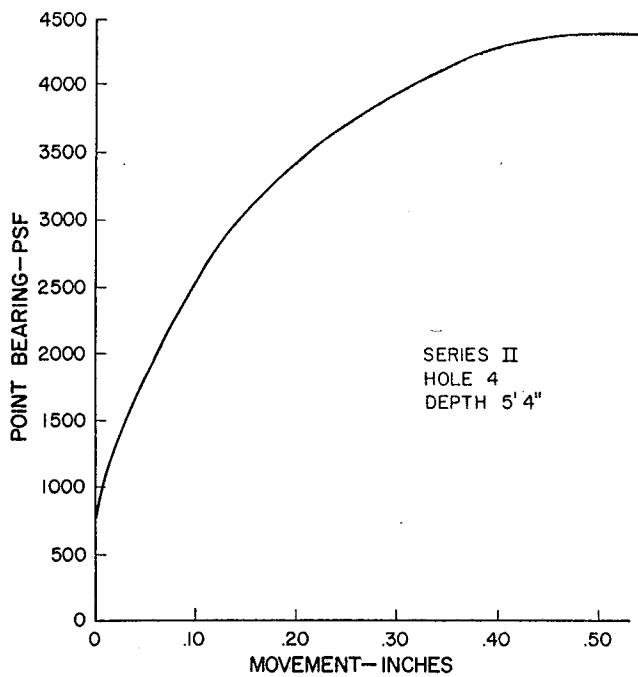

Figure A-8. *Point bearing vs movement curve.*

Figure A-9. *Total load vs movement curve.*

Figure A-11. *Point bearing vs movement curve.*

Figure A-10. *Skin friction vs movement curve.*

Figure A-12. *Point bearing vs movement curve.*

Figure A-13. Skin friction vs movement curve.

Figure A-15. Point bearing vs movement curve.

Figure A-14. Skin friction vs movement curve.

Figure A-16. Point bearing vs movement curve.
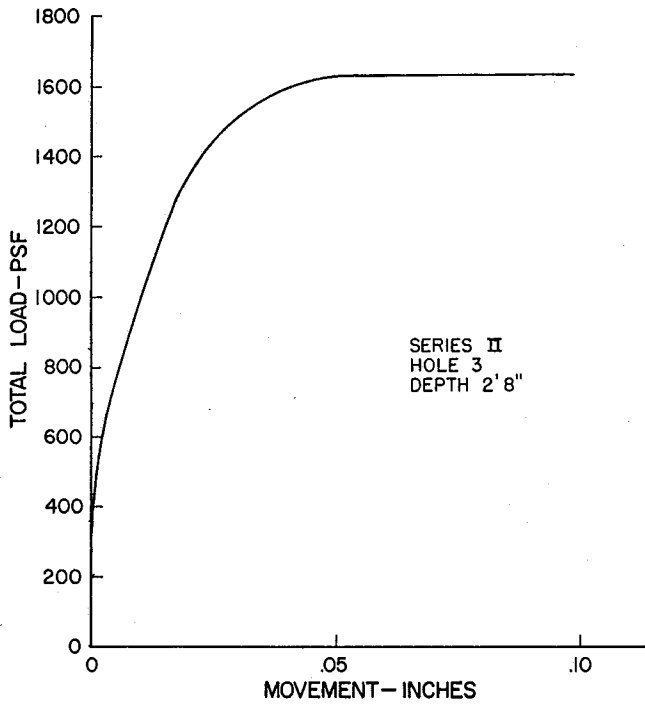
Figure A-17.   Total load vs movement curve.

Figure A-19.   Point bearing vs movement curve.

Figure A-18. Theoretical skin friction vs movement curve.

Figure A-20.   Total load vs movement curve.

Figure A-21. Theoretical skin friction vs movement curve.

Figure A-23. Total load vs movement curve.

Figure A-22. Point bearing vs movement curve.

Figure A-24. Skin friction vs movement curve.
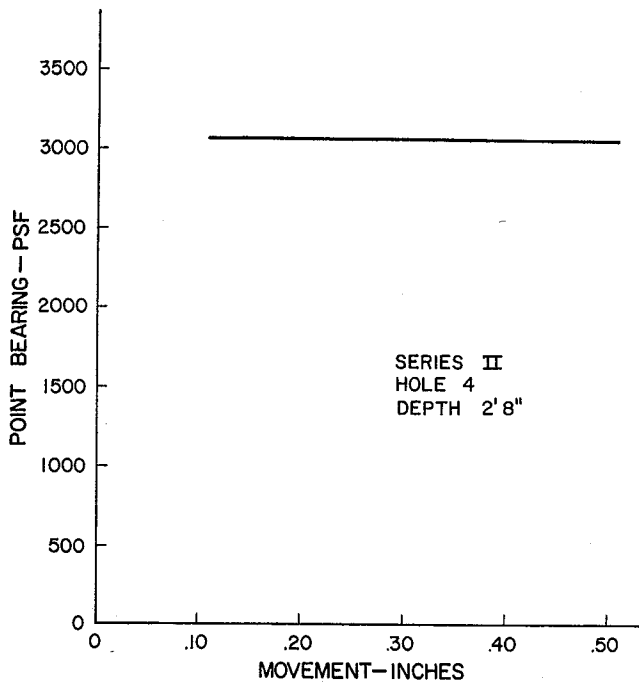
Figure A-25. Point bearing vs movement curve.
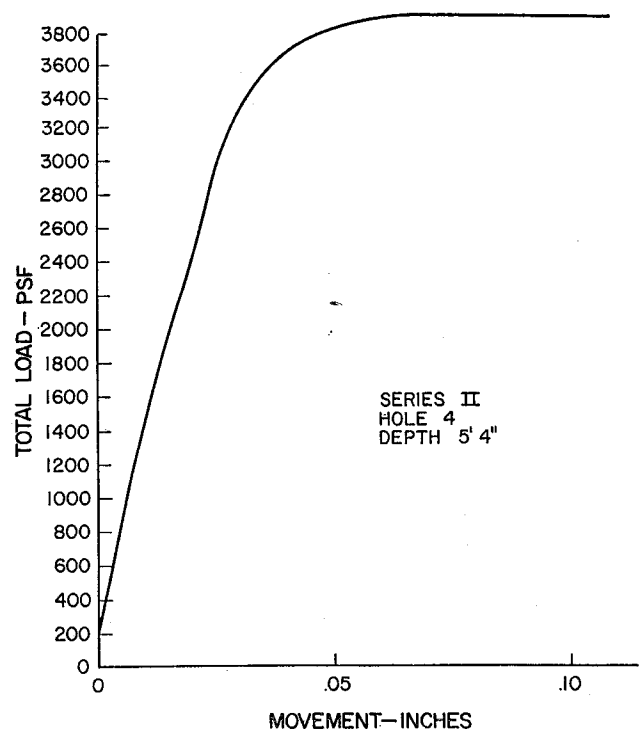
Figure A-27. Total load vs movement curve.

Figure A-26. Point bearing vs movement curve.
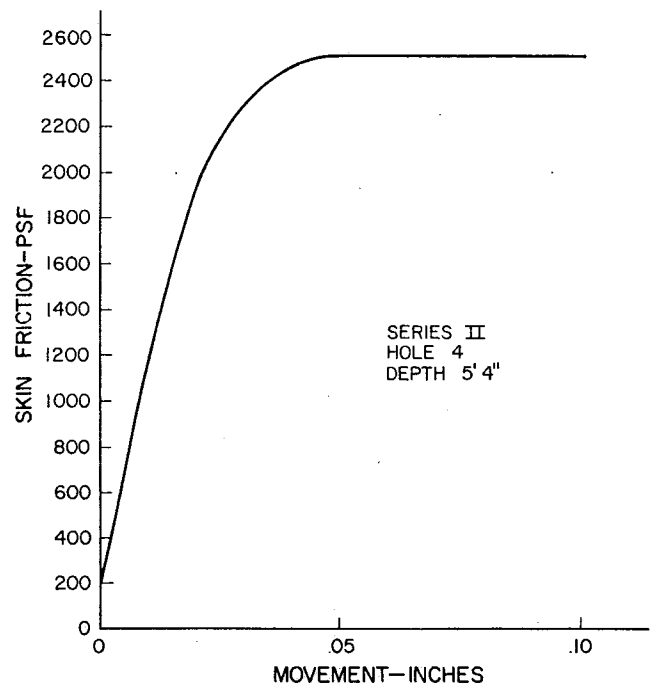
Figure A-28. Skin friction vs movement curve.
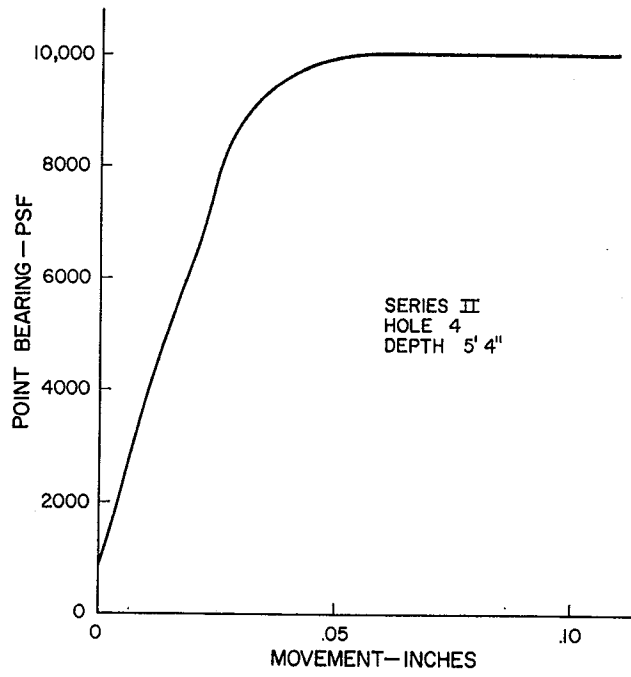
Figure A-29. Point bearing vs movement curve.

Appendix B

DYNAMIC LOAD DEFORMATION CURVES
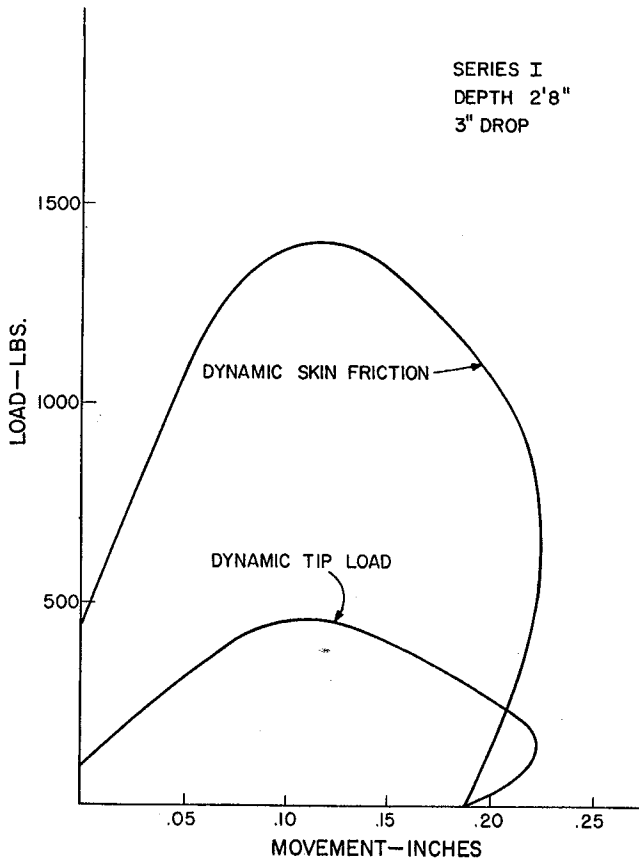
Figure B-1. Load deformation curves.
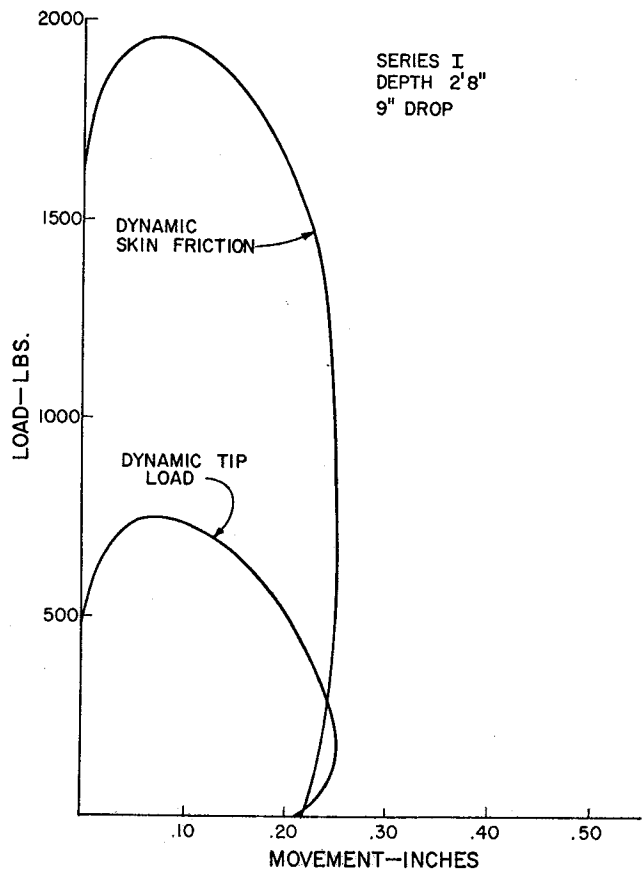
Figure B-2. Load deformation curves.
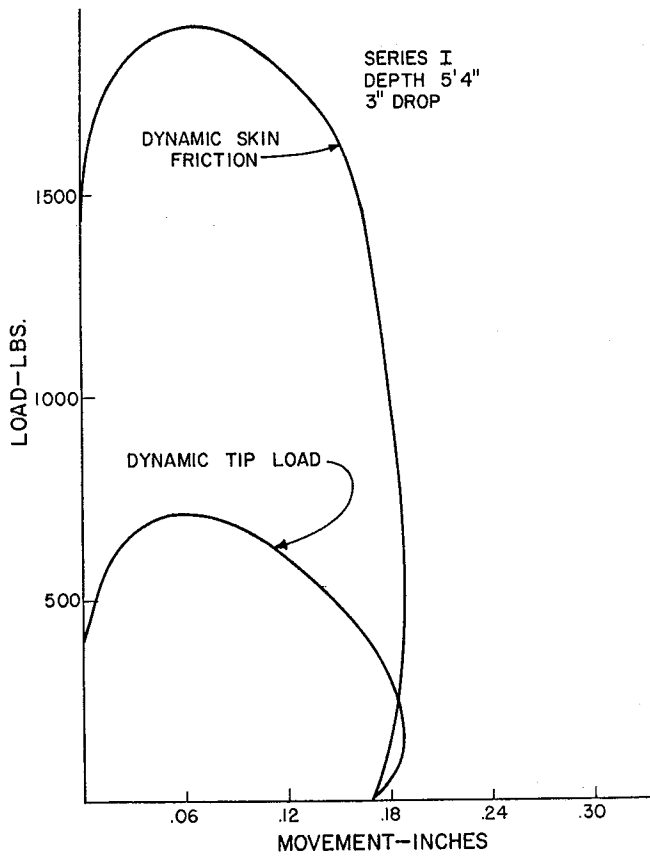
Figure B-3. Load deformation curves.
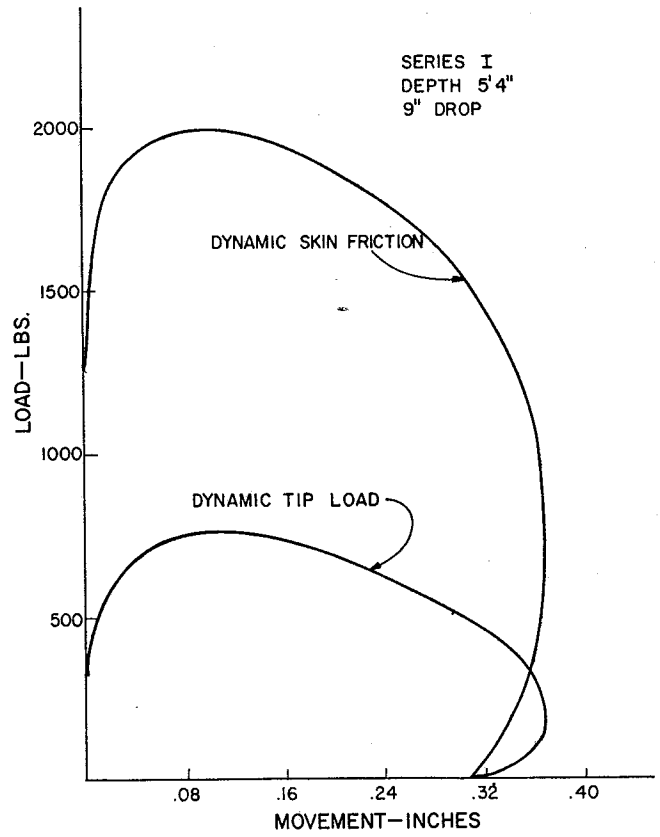
Figure B-5. Load deformation curves.
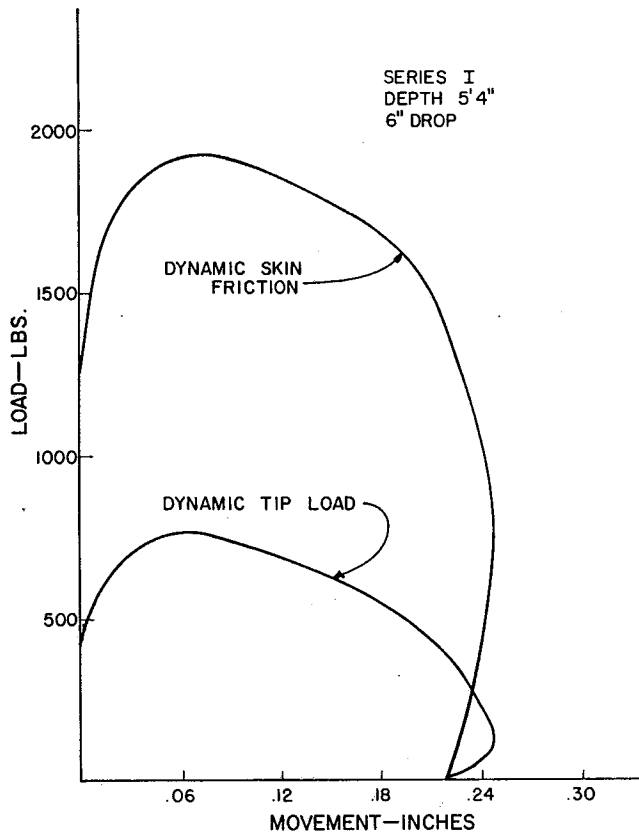
Figure B-4. Load deformation curves.
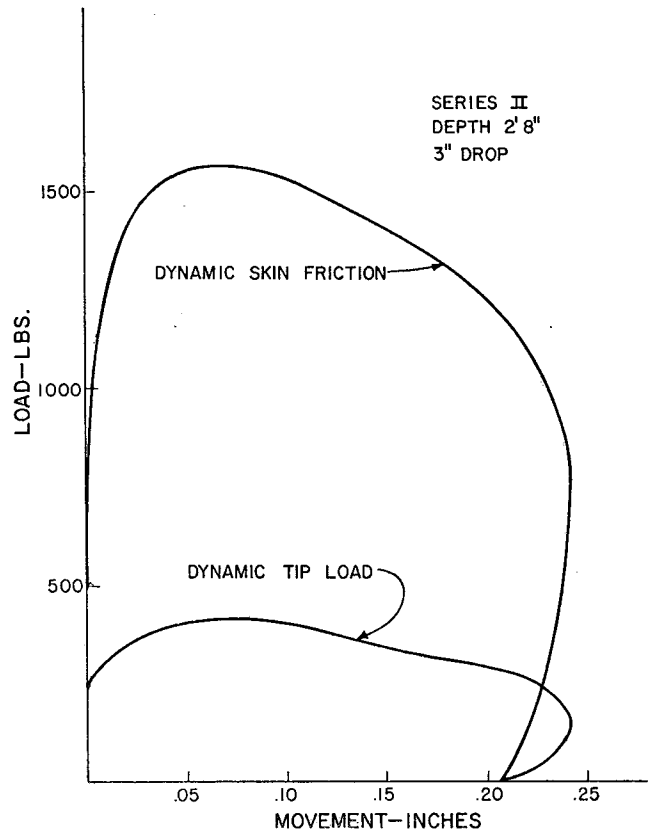
Figure B-6. Load deformation curves.
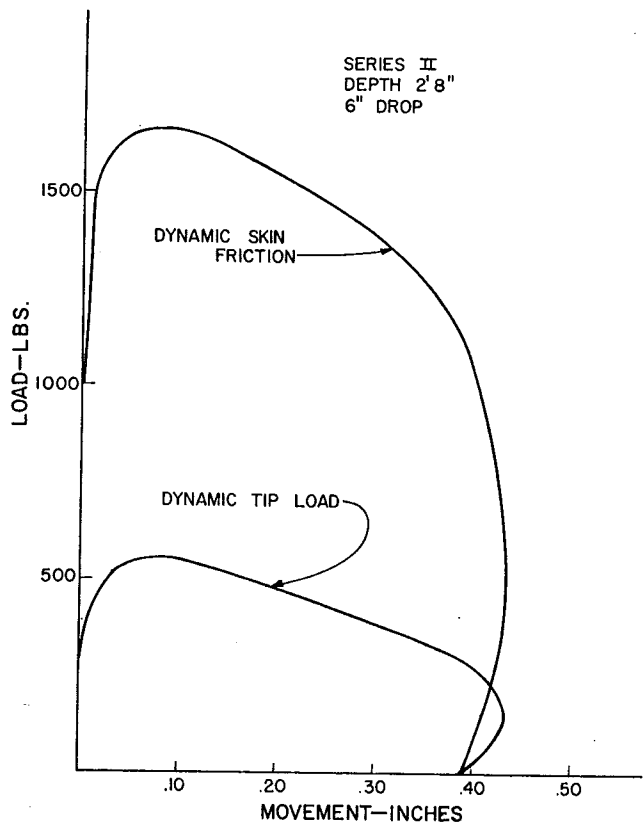
Figure B-7. Load deformation curves.
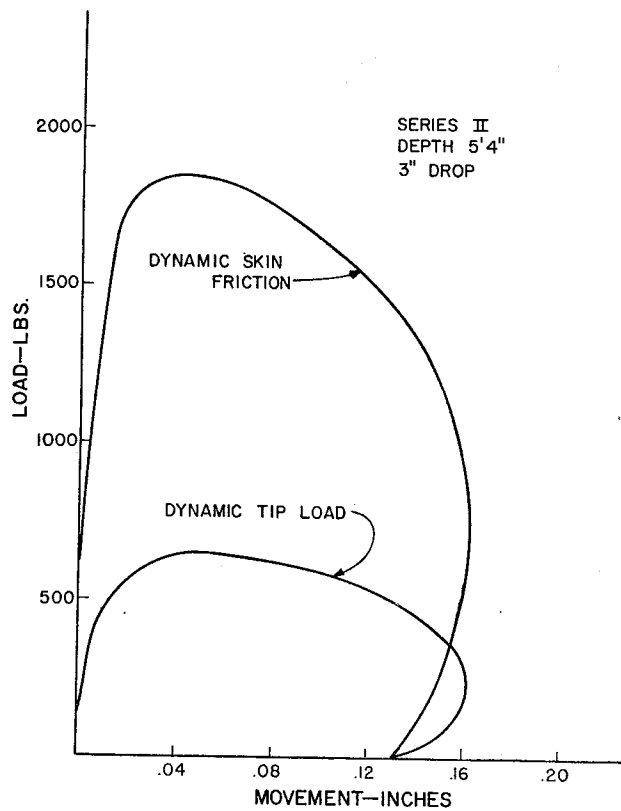
Figure B-9. Load deformation curves.
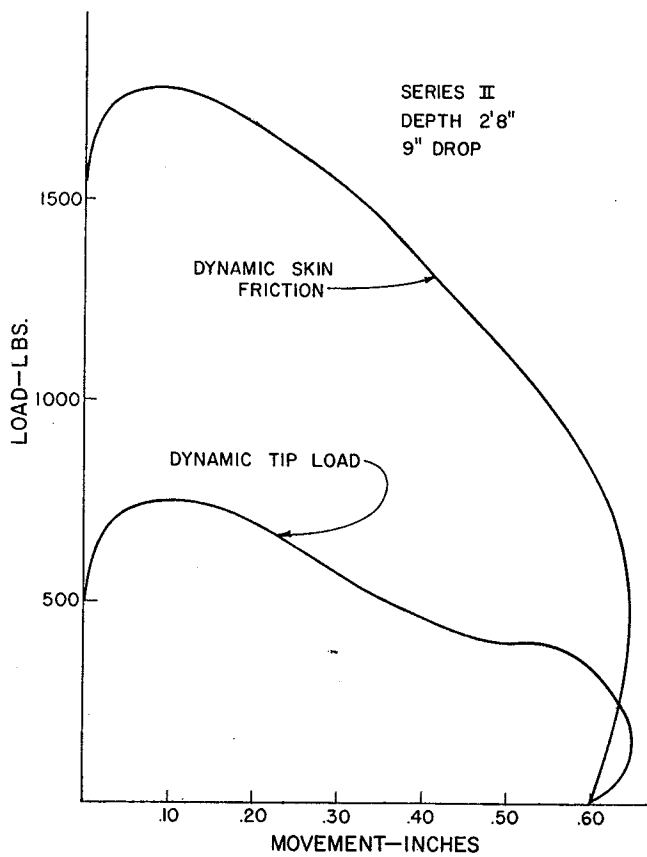
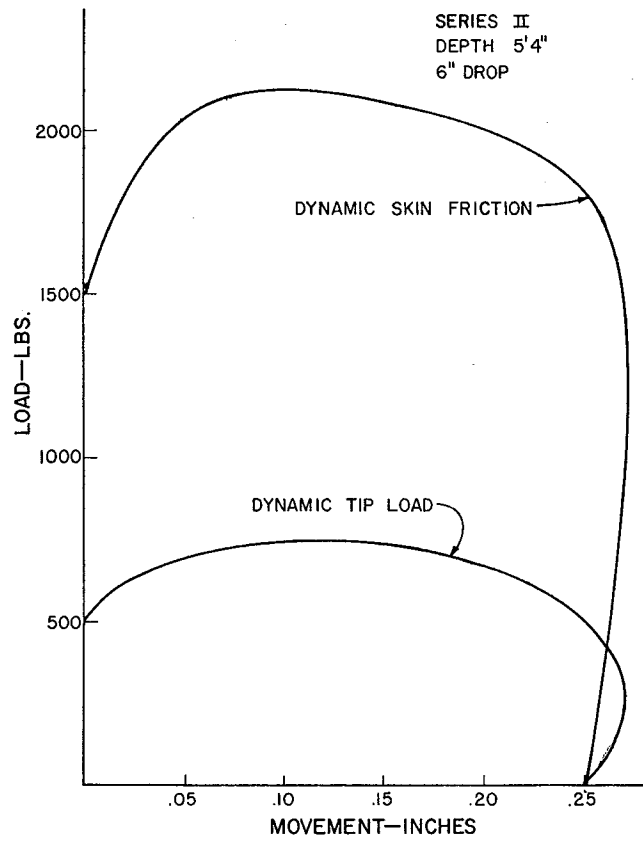*Figure B-8. Load deformation curves.*
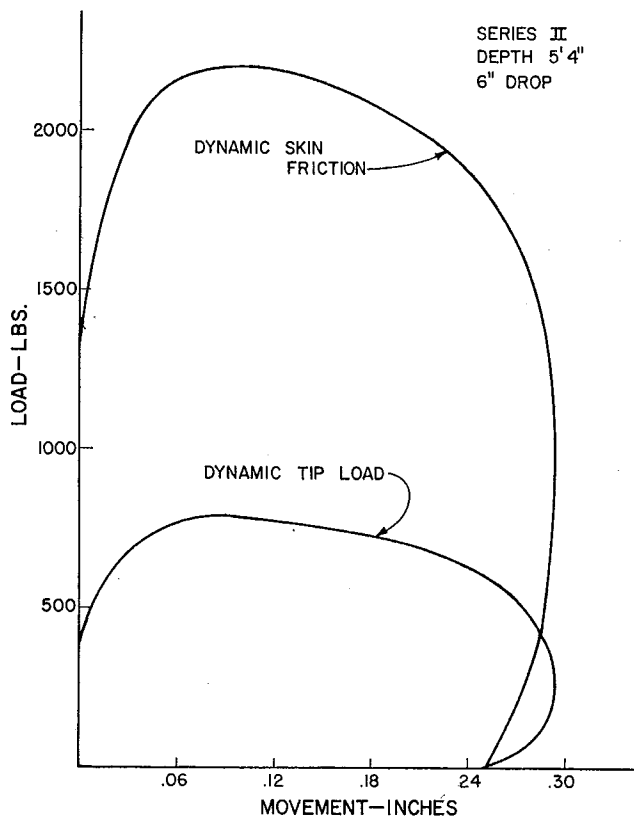
Figure B-10. Load deformation curves.

Figure B-11. Load deformation curves.

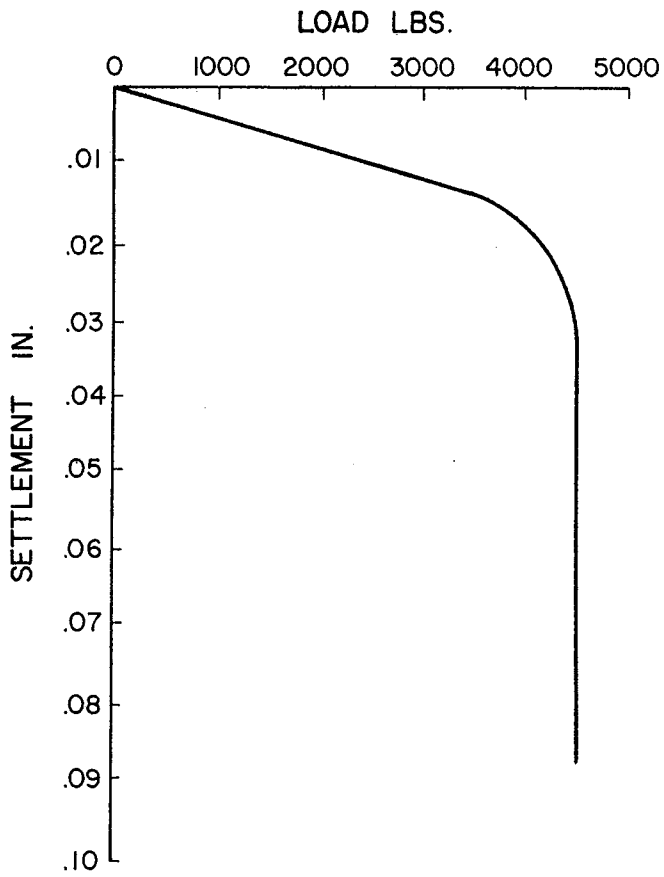# *Appendix C*

LOAD SETTLEMENT AND LOAD DISTRIBUTION CURVES

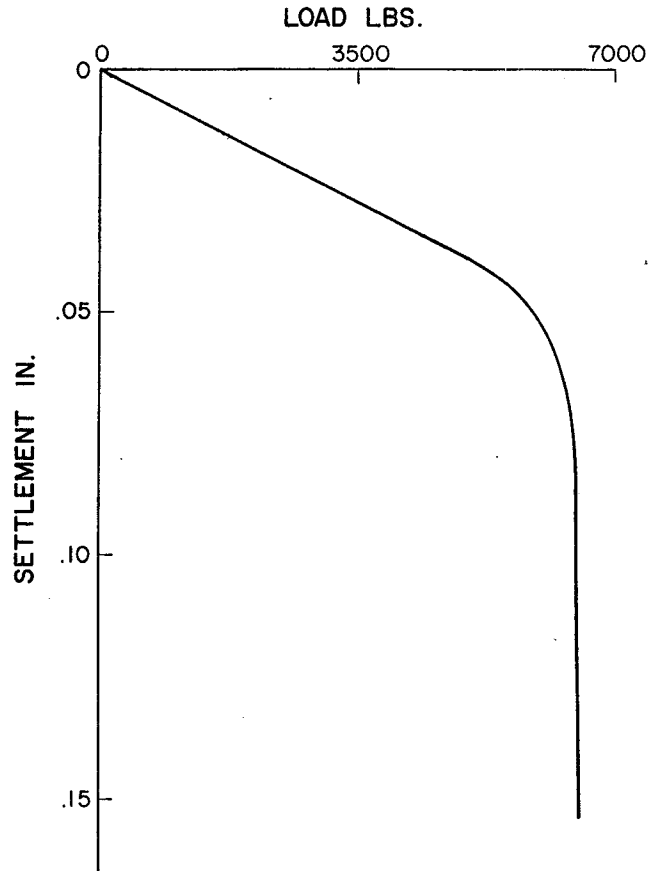Figure C-1.   Load vs settlement curve Test I-1-2.
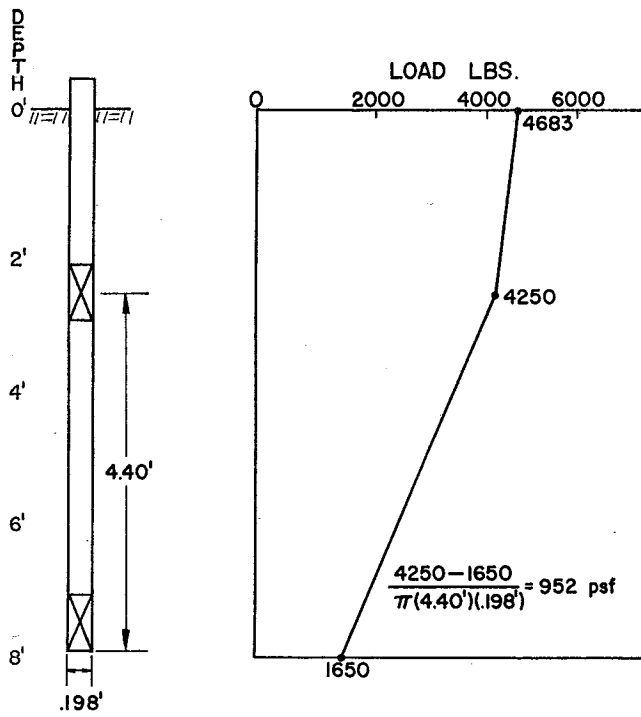

Figure C-2.   Load vs settlement curve Test II-1-1.

DEPTH

LOAD LBS.

4683

4250

$$\frac{4250 - 1650}{\pi(4.40')(.198')} = 952 \text{ psf}$$

1650

.198'

4.40'

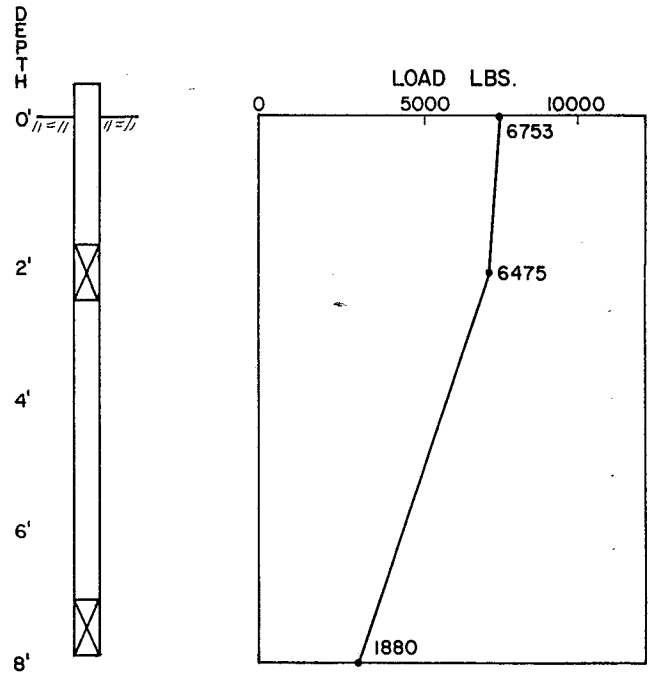*Figure C-3.   Load distribution at failure Test I-1-2.*

DEPTH

LOAD LBS.

6753

6475

1880

Figure C-4.   Load distribution at failure Test II-1-1.